## ABSTRACT

## TESTING OF SEMICONDUCTOR-BASED ADSORPTION MODIFIED PHOTOSENSITIVE (SAMP) SENSOR FOR RESPONSE TO TOLUENE

by
**Ashish Agrawal**

The response of semiconductor-based adsorption modified photosensitive sensor is based on the dye-enhanced photoconductivity of a CdS semiconducting film. The change in this photoconductivity is brought about when organic molecules are sorbed onto the dye-coated surface. The response is related to the overlap in the infrared spectrum of the dye with that of the analyte.

This research was carried out to study the response of the sensor to a typical hydrocarbon, toluene. The sensor was tested for its response to concentrations of toluene ranging from 2.6 ppm to 200 ppm in nitrogen. The sensor was tested under non-flow conditions and in the absence of oxygen and water vapor. Under these conditions, the Rhodamine B dye coated sensor was found to respond to changes in toluene concentration. The photoresistance of the sensor decreased as the concentration of toluene increased. The sensor showed high changes in photoresistance for lower toluene concentrations. Also, the rate of change of photoresistance was higher for higher concentrations of toluene. The sensor itself was very stable to long exposures to light but showed poor desorption characteristics. The sensor had to be flushed with nitrogen for extended periods to ensure complete desorption of adsorbed toluene.

This study forms the basis of future testing to be performed under more practical conditions, in the presence of water vapor and oxygen.

# TESTING OF SEMICONDUCTOR-BASED ADSORPTION MODIFIED PHOTOSENSITIVE (SAMP) SENSOR FOR RESPONSE TO TOLUENE

by
Ashish Agrawal

A Thesis
Submitted to the Faculty of
New Jersey Institute of Technology
In Partial Fulfillment of the Requirements for the Degree of
Master of Science in Chemical Engineering

Department of Chemical Engineering,
Chemistry and Environmental Science

January 2001

## APPROVAL PAGE

## TESTING OF SEMICONDUCTOR BASED ADSORPTION MODIFIED PHOTOSENSITIVE (SAMP) SENSOR FOR RESPONSE TO TOLUENE

**Ashish Agrawal**

---

Dr. Barbara B Kebbekus, Thesis Advisor — Date
Professor of Chemistry, NJIT

---

Dr. Somenath Mitra, Committee Member — Date
Associate Professor of Chemistry, NJIT

---

Dr. Basil C Baltzis, Committee Member — Date
Professor of Chemical Engineering, NJIT

## BIOGRAPHICAL SKETCH

**Author:** Ashish Agrawal

**Degree:** Master of Science

**Date:** January 2001

**Undergraduate and Graduate Education:**

- Master of Science in Chemical Engineering,
  New Jersey Institute of Technology, Newark, NJ, 2001

- Bachelor of Science in Chemical Engineering,
  University of Bombay, Mumbai, India, 1999

**Major:** Chemical Engineering

This thesis is dedicated to my family
for their unending love and encouragement.

## ACKNOWLEDGMENT

I start by expressing my sincere appreciation to my advisor, Dr. Barbara Kebbekus, for her dedication, patience, and wisdom throughout the length of this study and the preparation of this thesis, and without whose guidance this research would not have been possible. I am grateful to Dr. Somenath Mitra and Dr. Basil C Baltzis, who served as my committee members, for their inspirational and timely support, technical expertise, and acuity throughout the duration of the project.

I deeply appreciate the support given by Dr. Vladimir Zaitsev of Moscow State University, Moscow, Russia for providing the sensors for the study. A special mention has to be made of Mr. Yogesh Patel at New Jersey Institute of Technology for his help in use of resources and equipment. Without his help this study could not have been made.

## TABLE OF CONTENTS

## TABLE OF CONTENTS
## (Continued)

**Chapter** **Page**

## LIST OF FIGURES

**Figure** **Page**

## LIST OF FIGURES
## (Continued)

**Figure** **Page**

# CHAPTER 1

# INTRODUCTION

## 1.1 Overview

Everyday industry and other human activities release tons of gases into the atmosphere. Along with other components, these contain ozone precursors, VOC's such as benzene, toluene, ethylene, xylene and other olefinic compounds. If the quality of these gases is not kept under control, it can have disastrous effects. The government has imposed many laws and standards to curb this pollution. But identification of pollutants in these gases and their quantification is necessary before any decisions or actions can be taken.

Analysis of ozone precursors is a time consuming and expensive process. The methods used currently include trapping organics on packed traps, desorbing these organics either thermally or with a solvent and then carrying out gas chromatographic analysis often with mass spectrometric detection. Alternatively whole samples are collected in bulky stainless steel canisters and are concentrated on absorbent or cryogenic traps for gas chromatographic and mass spectrometric analysis. These methods though accurate are time consuming and cannot be done on-site. If real time data could be obtained, then feedback loops could be implemented to control the composition of exit gases. The Semiconductor based Adsorption Modified Photosensitive sensor is an attempt overcome these difficulties and provide a better alternative.

## 1.2 Chemical Sensing

Chemical sensing is part of an information acquisition process in which some insight about the chemical composition of a system is obtained in real time. In this process amplified electrical signals result from the presence of some chemical species. Generally chemical sensing consists of two distinct steps: recognition and amplification. Recognition is provided by some chemical means while amplification is provided by some physical means.

In general it is possible to distinguish two types of interaction of the chemical species: a surface interaction in which the species of interest is adsorbed at the surface, and bulk interaction in which the species of interest is adsorbed and partitioned between the sample phase and sensor [1]. The decrease of free energy is the driving force in all sensing processes.

## 1.3 Chemical Sensors

The purpose of a chemical sensor is to provide real-time reliable information about the chemical composition of its surrounding environment. Ideally, such a device is capable of responding continuously and reversibly and does not perturb the sample. For any sensor, important parameters include: response time, operating temperature range, sensitivity, selectivity (specificity), stability, low cost and reversibility. There are a variety of sensors available and each works on a different principle [1].

### 1.3.1 Thermal Sensors

Thermal sensors can be used for any process in which the internal energy of the system changes and is accompanied by absorption or evolution of heat. These sensors use the heat generated by specific reaction as the source of analytical information. In thermal sensors a chemically selective layer is placed on top of a thermal probe that measures the heat evolved during the specific chemical reaction taking place [2]. This is measured either as the change in temperature of the sensing element or the heat flux through the sensing element. The heat is evolved continuously, so thermal sensors are in a non-equilibrium state and their signal is obtained from a steady-state situation.

One variation of the thermal sensor is the catalytic gas sensor. In these sensors, heat is liberated during a catalytic reaction that takes place at the surface of the sensor. The related temperature change inside the device is measured. Catalytic gas sensors have been specifically designed for the detection of sub threshold concentrations of flammable gases in ambient air. Pellistors are sensors using a porous catalytic layer. But both, i.e. catalytic gas sensors and pellistors, are generally referred to as pellistors as a group.

### 1.3.2 Piezoelectric Mass Sensors

Piezoelectric devices are sensors which transmit acoustic waves through a solid substrate and are extremely sensitive to the adherence of mass to the surface of the device. Several types of acoustic piezoelectric devices are used as sensors. These types include quartz crystal microbalances, surface acoustic waveguides and others. When stress such as pressure is applied to such crystals the lattice is deformed and an electrical potential is

developed between the deformed surfaces. These devices are inexpensive to manufacture and can be fabricated in relatively small sizes (dimensions as few as mm). To obtain a sensor reading for a specific substance, the samples must first be separated into individual components or coatings must be placed on the sensor element to allow sorption of only selected substances.

In actual operation of the piezoelectric mass sensor, the application of an alternating potential difference to the crystals causes mechanical oscillations in the crystals at the natural resonant frequency [2]. The frequency is measured with a frequency meter and an appropriate electronic circuit. The deposition of a metal film (or any foreign substance) on the surface of the crystal causes a change in the frequency of oscillation of the quartz crystal. Piezoelectric sensors have found applications in chemical sensing particularly for gas and vapor sensing. The change in frequency is an indication of the amount of gas absorbed.

### 1.3.3 Fiber & Optical Waveguide Sensors

Waveguides are thin cylinders or flat segment of glass or plastic that transmit light by total internal reflection. Developed originally for telecommunication and optical computing applications, they have found another application in the analytical field as chemical and physical sensors. Optical sensors are a subset of waveguides. Fiber and waveguide sensors represent a dramatic shift from conventional sensors because fiber alternatives are potentially superior in terms of real time, in situ applications in remote locations. Furthermore these sensors represent a breakthrough in weight, size, and immunity to electromagnetic interference, sensitivity, and power requirement.

In optical sensors, a beam of light is guided out of the spectrophotometer, allowed to interact with the sample, and then reintroduced into the spectrophotometer in either its primary or secondary form for further processing. Waveguide chemical sensors employ chemical indicators for the sensitive and specific detection of analyte. The indicator can be incorporated on the tip or side of an optical fiber on a flat waveguide. The change in the intensity, lifetime, or phase of the light being transmitted forms the basis for selectivity and sensitivity[3].

Optical instrumentation can quantify the concentration of substances present in a sample by measuring the degree of electromagnetic radiation that is emitted, absorbed, fluoresced, or scattered by the substrate. Indications of the identity of the substrate can be obtained by determining the wavelength of radiation with which it interacts.

### 1.3.4 Electrochemical Sensors

Electrochemical sensors and detectors are very attractive for on-site monitoring of priority pollutants, as well as for addressing other environmental needs. Such devices satisfy many of the requirements for on- site environmental analysis. They are inherently sensitive and selective towards electroactive species, are fast and accurate, compact, portable and inexpensive.

In the case of electrochemical sensors, the analytical information is obtained from the electrical signal that results from the interaction of the target analyte and the recognition layer. Different electrochemical devices can be used for the task of environmental monitoring (depending on the nature of the analyte, the character of the sample matrix, and sensitivity or selectivity requirements). These include potentiometric

sensors (ion-selective electrodes, ion-selective field effect transistors and volumetric/amperometric sensors including solid electrolyte gas sensors. Most of these devices fall into two major categories (in accordance to the nature of the electrical signal): amperometric and potentiometric [4].

Amperometric sensors are based on the detection of electroactive species involved in the chemical or biological recognition process. The signal transduction process is accomplished by controlling the potential of the working electrode at a fixed value (relative to a reference electrode) and monitoring the current as a function of time. The applied potential serves as the driving force for the electron transfer reaction of the electroactive species. The resulting current is a direct measure of the rate of the electron transfer reaction. It is thus reflecting the rate of the recognition event, and is proportional to the concentration of the target analyte.

In potentiometric sensors, the analytical information is obtained by converting the recognition process into a potential signal, which is proportional (in a logarithmic fashion) to the concentration (activity) of species generated or consumed in the recognition event. Such devices rely on the use of ion selective electrodes for obtaining the potential signal. A permselective ion-conductive membrane (placed at the tip of the electrode) is designed to yield a potential signal that is primarily due to the target ion. Such response is measured under conditions of essentially zero current. Potentiometric sensors are very attractive for field operations because of their high selectivity, simplicity and low cost. They are, however, less sensitive and often slower than their amperometric counterparts.

# CHAPTER 2

# SEMICONDUCTOR-BASED ADSORPTION MODIFIED PHOTOSENSITIVE SENSOR

The development of highly sensitive gas sensors to provide continuous monitoring of the concentration of particular gases in the environment in a quantitative and selective way is an important issue. Current methods to analyze these gases include the use of sorbent traps and canisters, and these do not provide rapid information. Dr. Zaitsev and co-workers [5] at Moscow State University, Russia have been successful in developing sensors that address these issues. They have done so by investigating a new physical principle for building the selective gas sensors. The sensor selectively is due to the overlapping of rich vibrational spectra of gas molecules with those of the adsorbed dye and can be produced by depositing on the semiconductor surface, organic dye molecules with vibrational modes tuned to the vibration of those gas molecules. The information, graphs and diagrams provided here have been reproduced [5] with the permission of Dr. Zaitsev who served as a consultant for the research.

## 2.1 Description of Sensor

The most common types of semiconductor gas sensors are based on monitoring adsorption-induced changes in integral characteristics of the surface, such as dark- ($\sigma_d$) and photo- ($\sigma_p$) conductivity, or the surface potential Y. These integral characteristics are determined by equilibrium surface electron states (SES) that primarily depend on the structure of terminal chemisorbed molecular groups. Adsorption of atoms or molecules

on a semiconductor surface changes the distribution of existing, "biographical" surface electron states (BSES), and produces new adsorption surface electron states (ASES). In the case of Van-der-Waals adsorption, the energy parameters of BSES change only insignificantly. The energy spectrum of all states on a real disordered surface has a quasicontinuous nature and barely reflects the specificity of adsorbed molecules. All these factors restrict the variety of molecules that can be detected and result in extremely low selectivity of these sensors. The fabrication of selective commercial sensors involves surface modification or the use of catalysts.

The equilibrium response of the electronic semiconductor subsystem (variation of $\sigma_d$, $\sigma_p$, Y, etc.) to the adsorption process is traditionally believed to be a result of change in the occupation of its SES. This purely "charge-controlled" approach can hardly solve the selectivity problem. Dr Vladimir Zaitsev and co-workers [5] have tried to solve this problem by encompassing their efforts towards study of fine vibronic effects caused by adsorption. The issue can be successfully addressed by the combination of traditional semiconductor sensor techniques and fine vibronic effects caused by adsorption. An electron-vibrational coupling leads to a strong influence of the gas environment on photosensitization of electronic processes in semiconductors. Vibrational and rotational spectra of a molecule, considered as its signature, determine the vibronic interactions.

Photo-induced singlet-singlet $S_0 \rightarrow S_1$ transitions in the adsorbed dye molecules are known to initiate electronic transitions in solids. Two paths of such spectral sensitization are feasible: (i) resonant transfer of the reverse $S_1 \rightarrow S_0$ transition energy from a molecule to charged SES (Figure 1 a) and (ii) electron transition from an excited molecule to the solid conduction band (Figure 1 b).

In the first case the energy absorption cause an electron transition from SES to the conduction band. In the second case, molecule converted into an ion radical subsequently comes back into a neutral form trough charge carrier tunneling from the semiconductor. It was found out that in the insulator-semiconductor structures based on Ge and Si, only the first mechanism is taking place.

The overall deactivation rate constant ($k$) of the photoexcited molecule is determined by energy transfer through the following five channels: (1) luminescence ($k_l$); (2) nonradiative energy transfer to near adsorbed molecules through the Förster -Dexter induction-resonance mechanism ($k_{FD}$); (3) intermolecular singlet-triplet transfer ($k_{st}$); (4) electron-vibrational coupling (internal energy conversion to vibrational modes) ($k_{ic}$); (5) nonradiative energy transfer to the solid ($k_s$), i.e.:

$$k=k_l+k_{FD}+k_{st}+k_{ic}+k_s. \qquad (1)$$

In semiconductors, $k_s$ is determined by the efficiency of charge exchange between conductive band and different groups of surface electron states and by band-to-band transitions ($k_{BB}$):

$$k_s=k_{DT-}+k_{DT+}+k_{FS}+k_{SS}+k_{BB}, \qquad (2)$$

where $k_{DT-}$ and $k_{DT+}$ are the deactivation rates for electron and hole dielectric traps, respectively, $k_{FS}$, $k_{SS}$ - those for fast and slow electron states of the interface, respectively.

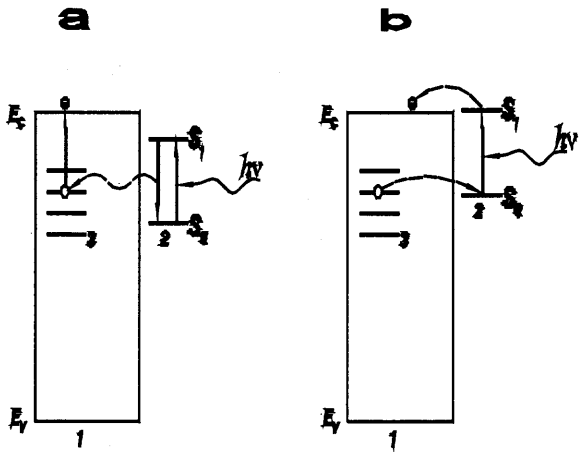


**Figure 1** Schematic diagram of two alternative mechanisms of spectral sensitization of electron molecules in the semiconductor by photo-excited sorbed molecules: (a) energy transfer. (b) electron transfer: $E_v$ and $E_c$ are the edges of valence and conductivity bands of dielectric, (1) dielectric, (2) adsorbed molecule, (3) charge traps in the insulator.
(Re- produced with permission from Dr. Zaitsev [5])

The experiments with the insulator-semiconductor structures built from Ge and Si show that energy transfer from donors (the excited dye molecules) to acceptors in a solid occurs by the dipole-dipole Förster-Dexter mechanism with a rate constant $k_{FD}$ given by:

$$k_{FD}=(R_0/R)^6 \cdot \tau_0^{-1}, \quad (3)$$

$R$ is the distance from donor to acceptor, $R_0$ is the critical radius (~5nm), and $\tau_0$ is the excited state lifetime of the isolated dye molecule. The same mechanism of energy transfer occurs in homogeneous molecular phase at low concentrations. The value of $\tau_0$ varies from 1.2 ns for monomers to 250 ns for dimers of RhB.

Combined electrophysical measurements of the surface charge and spectral measurements of molecular luminescence provide unique possibilities of studying fine vibronic effects in the semiconductor-dielectric-dye structures. The semiconductor electronic subsystem may be very sensitive to any changes in the adsorbed phase due to strong competition of two energy transfer channels: (1) inside the molecular phase (channel M) and (2) into semiconductor substrate (channel S). An intensive fluorescence quenching occurs and the SES emptying rate decreases, when molecules with overlapping luminescence and absorption bands are present on the surface. In case there is no resonance between electron transitions in molecular phase, the energy migrates through other alternative pathways in channel M: re-absorption of emitted photons and electron-vibrational coupling. In the latter case, the energy of a donor molecule excited electron transfers to vibrational modes of this molecule via internal conversion and then – to adjacent acceptor molecules if their vibrational spectra overlap.

## 2.2 Experiments by Dr. Zaitsev and co-workers

Dr. Zaitsev and co-workers [5] carried out experiments with single crystal germanium (Ge) and zinc oxide (ZnO) specimens as well as with polycrystalline ZnO and CdS films. ZnO films were prepared by oxidation of Zn films on an insulator substrate, and CdS films were deposited onto the insulator surface from water solution. Sapphire, quartz or glass substrates were used. Dye molecules of rhodamine B (RhB) or rhodamine 6G (Rh6G) were adsorbed on the surface of specimens from an ethanol solution. The surface concentration of rhodamine molecules was determined by means of a piezoresonance balance, and was chosen to be $2\times10^{13}$ molecules/cm$^2$ that made the efficiency of the channel S greater then that of channel M. SES in germanium – oxide structure was first charged by exposition of specimens to light. A xenon lamp and a monochromator was used to obtain the proper wavelength. A value of surface charge representing the electron subsystem response in Ge was measured by the field-effect on a high sinwave signal – the standard method for measuring semiconductor surface potential. In ZnO and CdS the electron subsystem response was detected as a change in photoconductivity. In order to obtain photosensitized effects, the specimens were illuminated with monochromatic light to excite the dye molecules. To study an influence of ambient gases the samples were exposed to a low-pressure vapor of naphthalene and ethanol, as well as deuterated naphthalene. The molecular electronic spectra of these species differ substantially from those of RhB, while vibrational spectra of CH groups in ethanol and naphthalene molecules partially overlap with some vibrational modes of RhB. The vibrational modes in deuterated molecules are shifted, thus no resonance transfer is expected.

## 2.3 Results obtained by Dr. Zaitsev and co-workers

Dr. Zaitsev and co-workers [5] found that the results were similar for all studied systems. Consider an effect of naphthalene molecules on the RhB fluorescence. In the presence of naphthalene, the RhB fluorescence was quenched and a broadening of the spectrum by $\Delta\lambda$=87% was observed. According to formulas (1) and (2), this can be explained only in terms of electron-vibrational coupling in RhB molecule because the strong mismatch of the naphthalene and RhB electron spectra does not allow the direct electron energy transfer. The presence of the deuterated naphthalene molecules, with vibration modes that differ from those of naphthalene, produced neither fluorescence quenching, nor broadening of the spectrum. This fact confirmed the resonant vibronic nature of the observed phenomenon.

Electron traps in the oxide phase were filled with carriers injected through the interface of the semiconductor and the substrate, when the structure was illuminated with photon energy exceeding potential barrier of the interface $hv \geq Wp$=2 eV. The maximum value of the charge, $\Delta Q_{smax}=1.5\times10^{11}$ electron charges/cm$^2$, was observed at hv=3.2 eV. Existence of RhB molecules on the $GeO_2$ surface did not change the spectrum and the value of the surface charge.

The surface charge requires about 30 min in darkness before relaxing to a stable value. If, after charging, the specimen were additionally illuminated in the RhB absorption band, the surface charge relaxation rate increased.

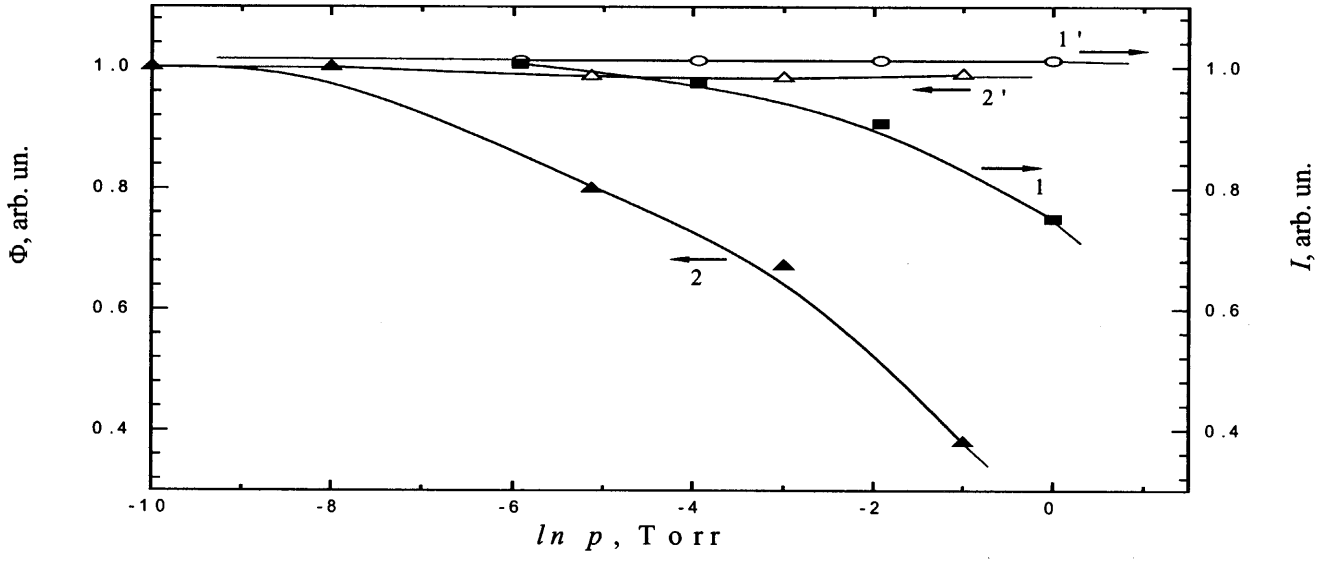


**Figure 2** Fluorescence intensity of rhodamine B(1,1') and efficiency of SES photo discharge(2,2') in Ge-GeO2-RhB system as a function of naphthalene and the deuterated naphthalene (1',2') vapor pressure. The SES photo discharge date were extracted from the surface potential measurements. (Re-produced with permission from Dr. Zaitsev [5])

This effect is related to the additional photosensitized emptying of traps in the dielectric at the expense of the electronic excitation energy of the RhB molecules. Dr. Zaitsev and co-workers [5] apply the term "efficiency of SES photo-emptying" to quantity $\Phi=(Q_0-Q)/Q_0$, where $Q$ and $Q_0$ are the surface charge remained after 10-minute relaxation under and without an additional illumination in the absorption band of the dye, respectively. Experiments showed that no photo ejection happened if the structure, either with a dye or without, were exposed to light outside the absorption band.

Adsorption of the naphthalene molecules significantly reduces the value of $\Phi$ owing to vibrational deactivation of some RhB molecules. Figure 2. shows the decrease of the parameter $\Phi$ and the intensity of luminescence $I$ versus naphthalene vapour pressure. No effect was observed in the presence of the deuterated naphthalene molecules.

Intercombinative conversion in RhB molecules is rather insignificant, and there is no change in the rate constant of energy transfer by the inductive-resonance mechanism from the RhB to the guest molecules. Hence the observed quenching of RhB fluorescence and the change in the efficiency of the photo-ejection can only be attributed to the internal conversion of the electronic excitation of the RhB molecules to vibrational modes accompanied by subsequent energy transfer to the guest molecules. In their experiment, the distance between the RhB molecules at the Ge surface were large (~5 nm), and there was almost no energy transfer between them. Therefore, the high sensitivity of $I$ and $\Phi$ to the guest molecules can only be attributed to the fact that their vibration mode energy comes very closely to the vibration energy of the RhB molecules interacting with them. The fact that the system shows no sensitivity to deuterated

molecules indicates that the vibrational modes of the interacting molecules must be the same.

Of the two discussed parameters, $I$ and $\Phi$, the latter has proved to be more sensitive to the presence of guest molecules. This implies that the electrophysical method is more promising for gas detection than the optical one. It provided a basis for sensors tested in this work, which depend for their operation on the vibrational deactivation of photoexcited adsorbed dye molecules in the presence of gas molecules. Furthermore, this will substantially extend the class of detectable molecules, including isotopically substituted ones. Dr. Zaitsev and co-workers [5] observed similar effect with $H_2O$, $D_2O$ earlier.

The observed influence of vibronic effects in the semiconductor-insulator-dye system on its electronic subsystem was found to be rather strong. Dr. Zaitsev and co-workers [5] have performed similar experiments using a popular material for photosensitization studies: zinc oxide single crystals and polycrystalline films with rhodamine molecules adsorbed on the surface. First, they found that RhB adsorption and the subsequent naphthalene absorption did not change the dark conductivity. Molecules of these organic compounds are tied to the surface by weak dispersion forces and do not substantially alter the BSES. Figure 3 shows spectral dependencies of the photoconductivity of ZnO specimens without and with adsorbed dye. The photoconductivity spectra of ZnO crystals represents a sharp edge of fundamental absorption at $h\nu$=3.3 eV, i.e. at the energy corresponding to the gap of ZnO (Figure 3, curve 1). Here $\sigma_p$ is the ratio of the photo- and dark conductivity. This edge smears for the polycrystalline film.

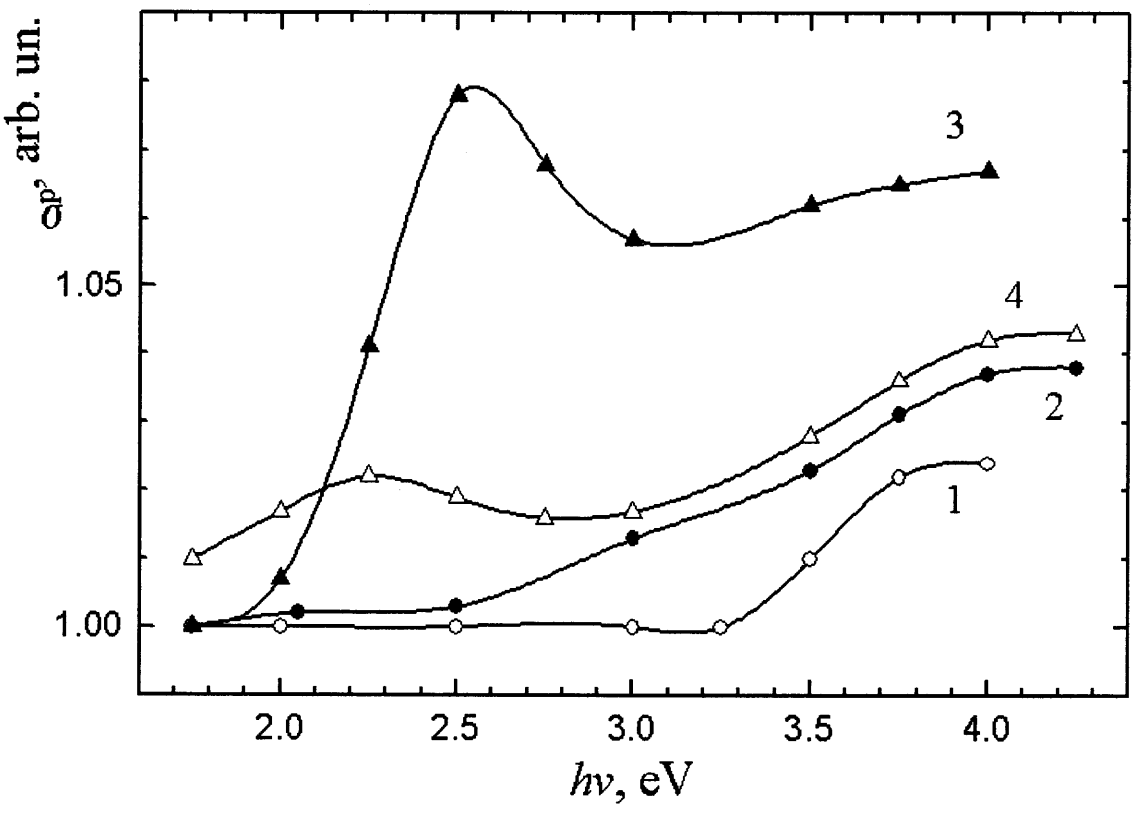


**Figure 3** Photoconductivity spectra of single crystal (1,3) and polycrystalline(2,4) ZnO without dye(1,2) and after RhB deposition(3,4). (Re- produced with permission from Dr. Zaitsev [5])

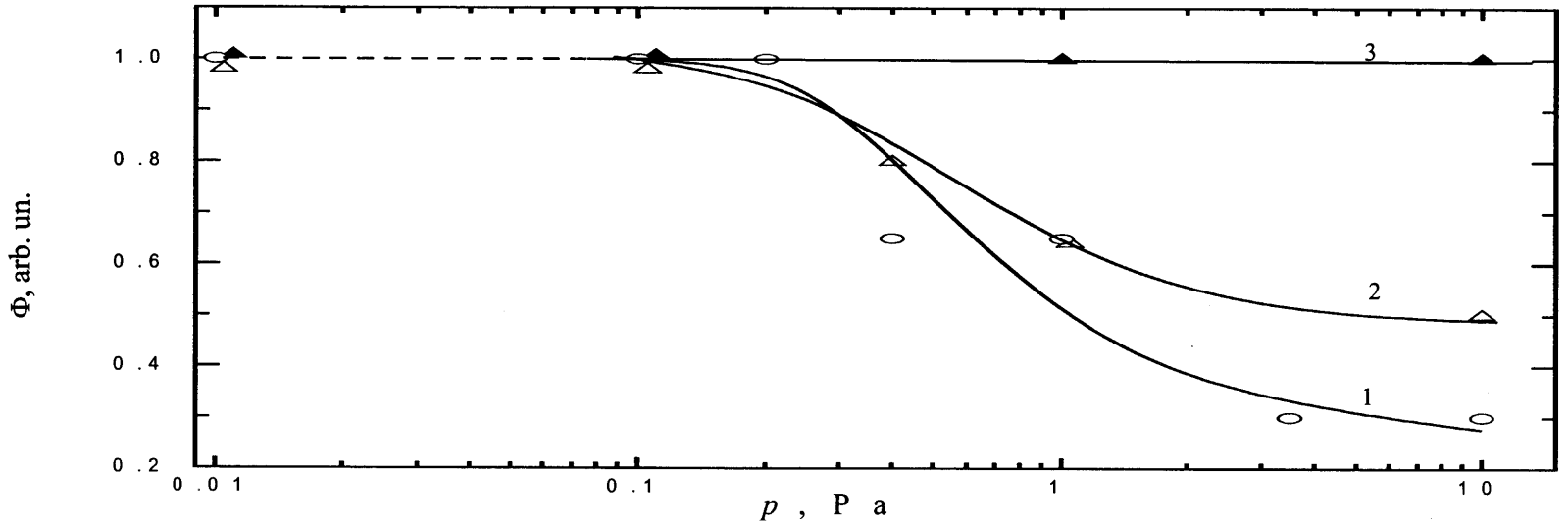


**Figure 4** Efficiency of conductivity photosensitization as s function of naphthalene vapor pressure for ZnO single crystal (1) and polycrystalline film (2) with adsorbed RhB molecules. The same: with deuterated naphthalene (3). (Re-produced with permission from Dr. Zaitsev [5])

When a crystal with dye adsorbed was placed in vacuum and illuminated in the spectral range of RhB absorption, hv=2.3-2.5 eV, Dr. Zaitsev co-workers observed a typical spectral sensitization effect was observed, that is the steep increase in $\sigma_p$. This effect is less prominent for the polycrystalline film.

Admission of naphthalene vapors to the surface reduced the sensitization efficiency. The effect was observed when the naphthalene vapor pressure exceeded the value of 0.1 Pa. Figure 4 demonstrates the pressure dependence of the ratio $\Phi = \sigma_p/\sigma_{p0}$. The terms in the expression are $\sigma_{p0}$ and $\sigma_p$, which are the values of photoconductivity at the maximum of the RhB absorption band before and after adsorption of the 'guest' naphthalene molecules respectively. The electronic spectrum of adsorbed naphthalene molecules are shifted to the higher frequencies compared to RhB spectrum. The sensitization efficiency reduction of the photoconductivity of ZnO may be attributed only to the higher rate of other competing energy transfer channels from photo excited RhB molecules, such as the channel of vibration resonance transfer.

Sensor systems consisting of Ge-$GeO_2$ or ZnO base with adsorbed rhodamine molecules showed high sensitivity to such hydrocarbons as naphthalene. High selectivity of tested sensors to hydrocarbons is due to resonance of molecular vibration modes. However, the systems based on Ge-$GeO_2$ and ZnO were found to have a sensitivity to water vapor which would decrease the sensitivity to organic molecules under atmospheric conditions. Therefore a system based on thin polycrystalline film of CdS with adsorbed dye molecules was selected for further testing.

Spectra of dark and photoconductivity of CdS films of different thickness and grain sizes were similar to those of ZnO shown in Figure 3. The band of sensitized

conductivity due to RhB molecules had maximum at 2.3 eV. The conductivity of the films tested was only slightly dependent on water vapor concentration allowing hydrocarbon measurements under real atmospheric conditions. Admission of naphthalene and ethanol vapors to the chamber with sensor changed the photoconductivity over a wide region of light energies. However, the system was much more sensitive to the ambient hydrocarbon concentration in the band due to RhB molecules presence, where the sensor is very selective because of vibration resonance. The system response spectra to naphthalene and ethanol vapor is shown on Figure 5. The coefficient of photoconductivity reduction was taken as $K = \sigma_p/\sigma_{p0}$, where $\sigma_{p0}$ and $\sigma_p$ are the values of photoconductivity before and after adsorption of the 'guest' molecules respectively. The Figure 5 shows that system response at the RhB absorption band was 5 to 10 times higher than in intrinsic photoconductivity band of CdS. The response to ethanol vapors is stronger because the higher vapor pressure of ethanol is 400 times higher.

Thus Dr. Zaitsev co-workers [5] have investigated a new physical principle for building selective gas sensors. The sensor selectivity in this case is due to the overlapping of rich vibrational spectra of gas molecules with those of adsorbed dye. The selective sensor for specific gas molecules could be produced by depositing on the semiconductor surface organic dye molecules with vibrational modes "tuned" to the vibration of those gas molecules. Water and naphthalene isotopes can be distinguished in this way, which could not be done with traditional chemiresistors. The results obtained with "CdS – adsorbed dye" systems are especially promising in terms of new design for gas sensors based on physical principles of selectivity. Modern organic synthesis offers ample scope for building systems with vibration modes selective to specific gas molecules.

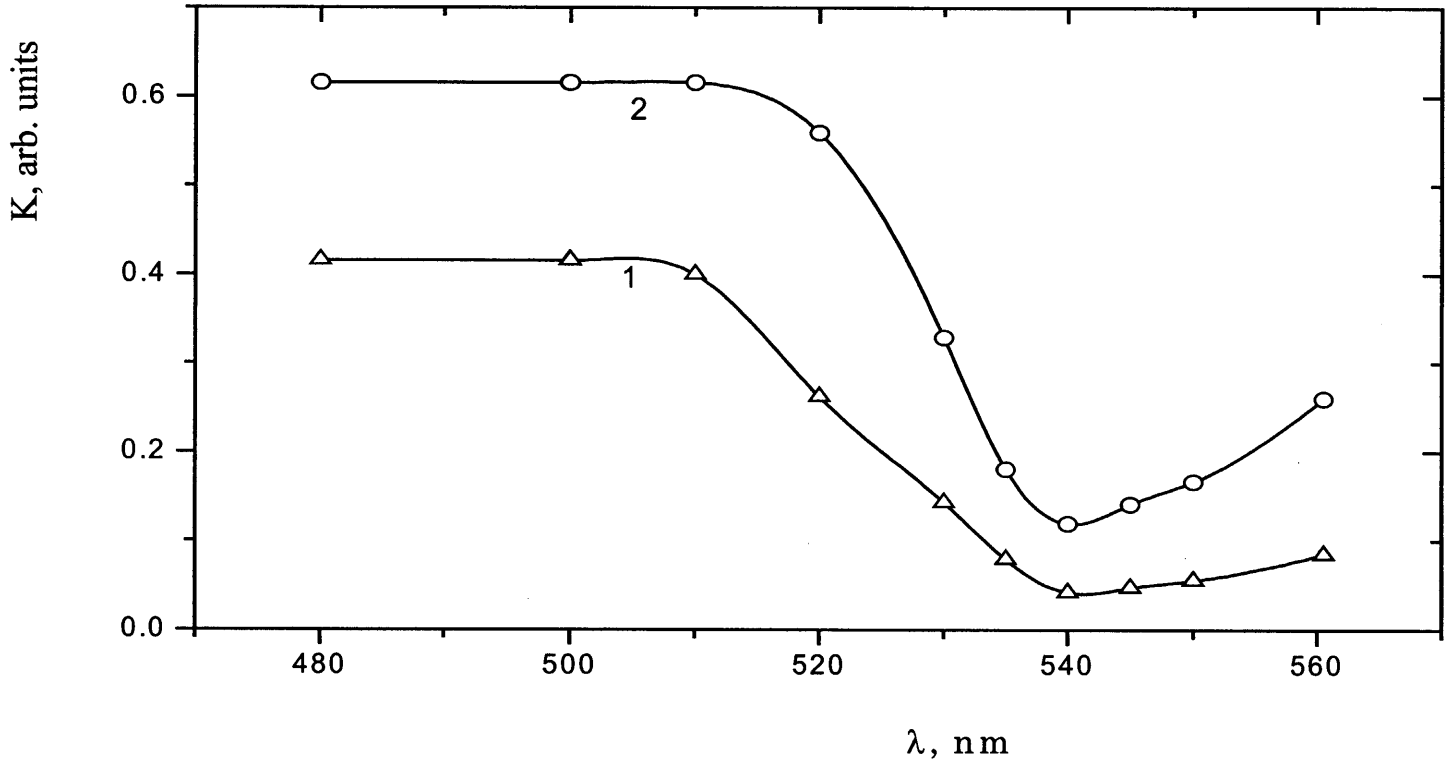


**Figure 5** Spectral dependence of the coefficient of photoconductivity reduction by ethanol vapor pressure p = 400Pa (1) and naphthalene vapor of p=1 Pa (2) for CdS film with adsorbed RhB molecules. (Re-produced with permission from Dr. Zaitsev [5])

# CHAPTER 3

# EXPERIMENTAL METHODS

Experiments were carried out to demonstrate that the sensors responded to different concentrations of toluene in nitrogen at atmospheric pressure. Toluene was selected as a typical aromatic compound. The sensors had been tested by Dr. Zaitsev and co-workers [5] for low-pressure vapors for pure naphthalene. The objective of this study was to test the sensors for toluene under atmospheric conditions and for a wide concentration range of toluene. The experimental set up was designed to test the sensors keeping in mind that the sensor had to be exposed to monochromatic light.

## 3.1 Experimental Apparatus I

Initially, experiments were carried out to ensure that there was indeed a change in the resistance of the sensor when it was exposed to light in a hydrocarbon free environment v/s when exposed to light in the presence of toluene.

### 3.1.1 Apparatus

In order to achieve this, the experimental set up shown in Figure 6 was used. As can be seen in the figure, the sensor was placed in a glass bulb and the light filter was supported above the sensor by means of a stand. Light was placed on top of the broadband (500 nm) filter. The system for filling the bulb with test gas mixture was designed to be a continuous process with provision for a batch process. There were two alternate paths

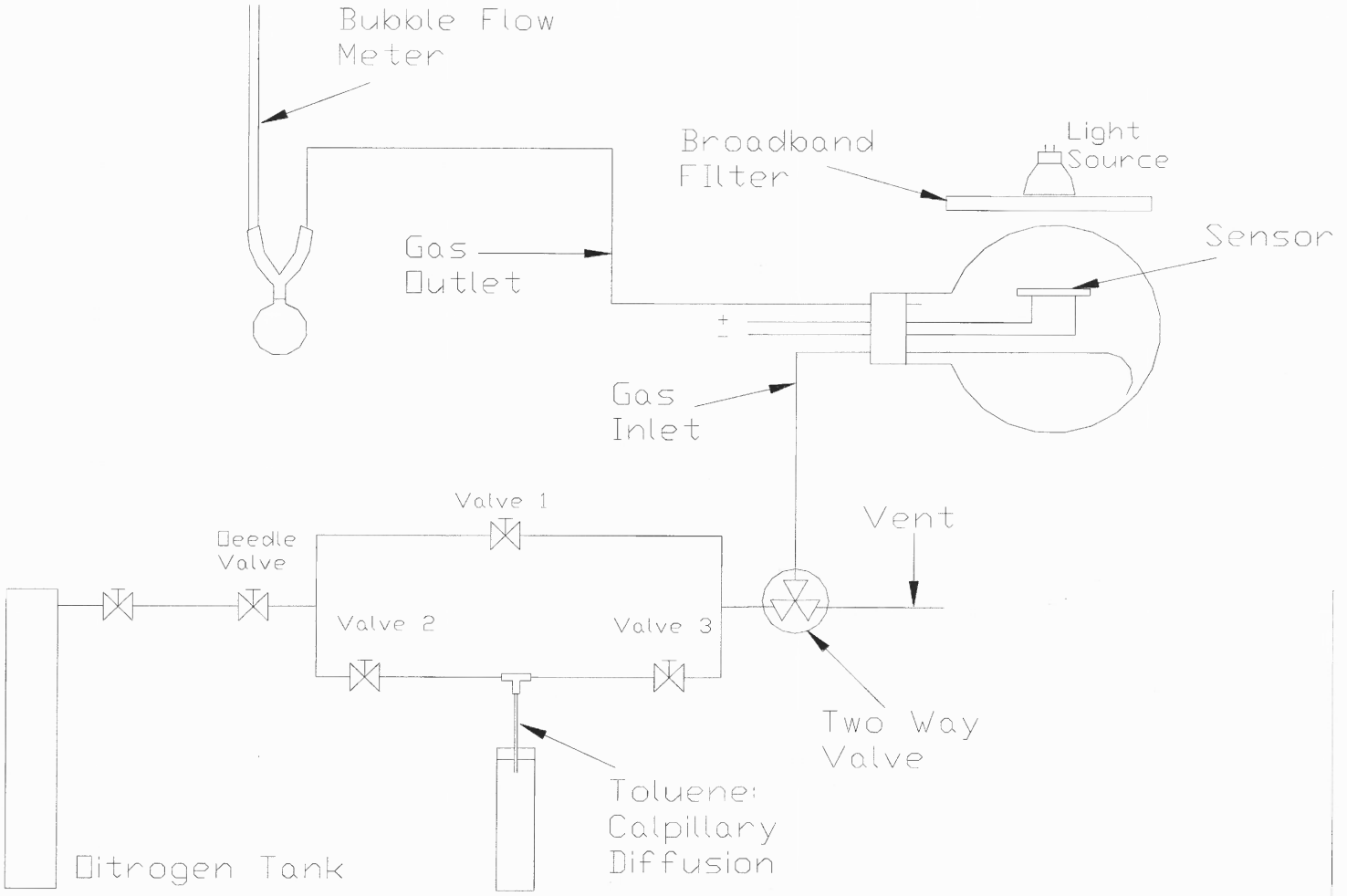


**Figure 6** Schematic of Experimental Set-Up I

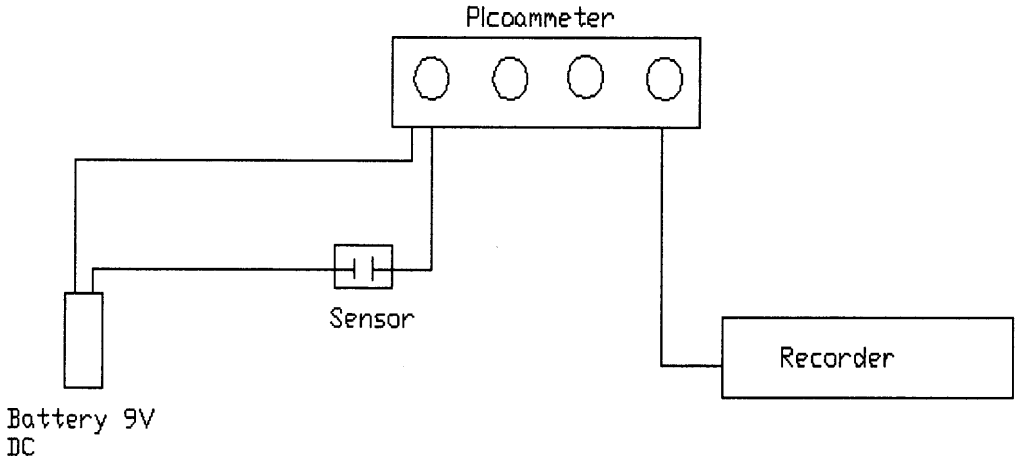


**Figure 7** Electrical Circuit for the sensor

that nitrogen could take. One was used to flush the bulb with nitrogen. The other path included a toluene diffusion system. Toluene diffusing through the capillary was entrained in the nitrogen giving a gas stream of a particular concentration as described in section 3.1.2.

A two-way valve was used to switch the nitrogen flow between the vent and the flask. The rubber stopper to the flask had inlet and outlet tubings (stainless steel 1/8th inch in diameter) for the gas. In order to measure the flow rate, a bubble flow meter was attached at the exit. The rate at which the bubble rises in the calibrated tube gives the gas flow rate. A needle valve was used to control the flow of nitrogen. The sensor was supported on copper wires in the round bottom flask. The wires connected the sensors to the 9V battery source and the picoammeter, as shown in Figure 7.

### 3.1.2 Capillary Diffusion

Capillary diffusion was used to introduce toluene into the nitrogen flow as it was being let into the flask. The concentration of toluene in the nitrogen stream depends on the flow rate of nitrogen, the temperature of the toluene and the size of capillary. For all initial experiments the same combination of these factors was used. The size of capillary used was 0.02" inner diameter. The equation, as specified in the ordering information for capillaries by VICI Metronics Inc., Santa Clara, CA, was used to calculate diffusion the through the capillary and is as follows:

$$r = 1.9 \times 104 \times T \times D_o \times M \times (A/L) \times \log [P/(P-p)]$$

where, r = rate of diffusion in mg/min

T = temperature of vapor in K = 293 K

$D_o$ = diffusion coefficient at 25 °C, 1atm = 0.088 $cm^2$/sec at 30 °C

M = molecular weight in g/mole = 92.14

A = cross section of capillary in $cm^2$ = 20.268 X $10^{-4}$ (0.02" capillary)

L = length of diffusion path in cm = 5 cm

p = atmospheric pressure in mm Hg = 760mm Hg

P = vapor pressure of toluene at temperature T in mm Hg = 20.38 mm Hg

This resulted in a rate of diffusion of 2.48 x $10^{-9}$ gmoles/min. A nitrogen flow rate of 13 ml/min produced a toluene concentration of 4.4 ppm in the nitrogen stream. The concentration of toluene in the flask increases from 0 at the start and approaches 4.4 ppm exponentially as shown in Figure 8.

If there was no nitrogen flow and the toluene was allowed to diffuse into the space between valves 2 and 3 (Figure 6) then the toluene concentration between the two valves would reach a saturation concentration of 30325 ppm. When this saturated stream was introduced into the flask, it resulted in an initial concentration of 2000 ppm in the flask. Thus, with initial flask concentration of 2000 ppm followed by a continuous flow of nitrogen containing 4.4 ppm toluene, the concentration in the flask would decrease exponentially from 2000 ppm to 4.4 ppm of toluene as shown in Figure 9.

### 3.1.3 Procedure

Before each run, the flask was first washed with soap solution to ensure that there was no residual toluene in the flask from previous run. Also the rubber stopper of the flask was slightly heated with a heat gun to desorb all the toluene. The flask was then flushed with

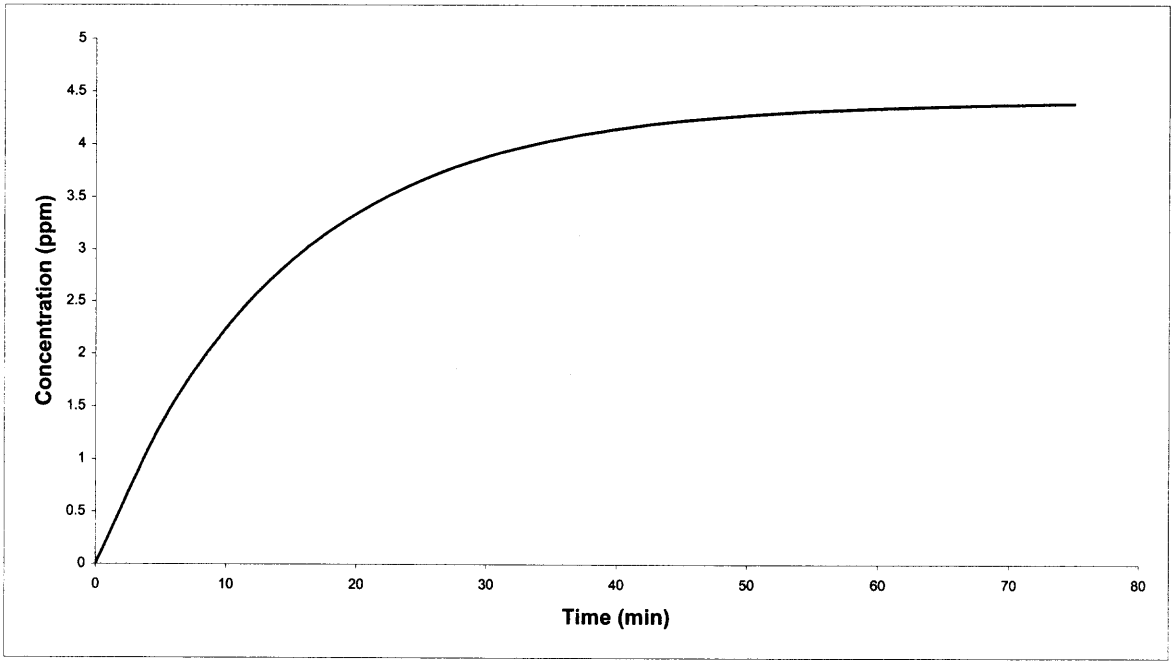


**Figure 8** Change in Concentration of Toluene in the flask vs. time when 4.4 ppm toluene mixture is passed into flask containing nitrogen, at 13 ml/min.

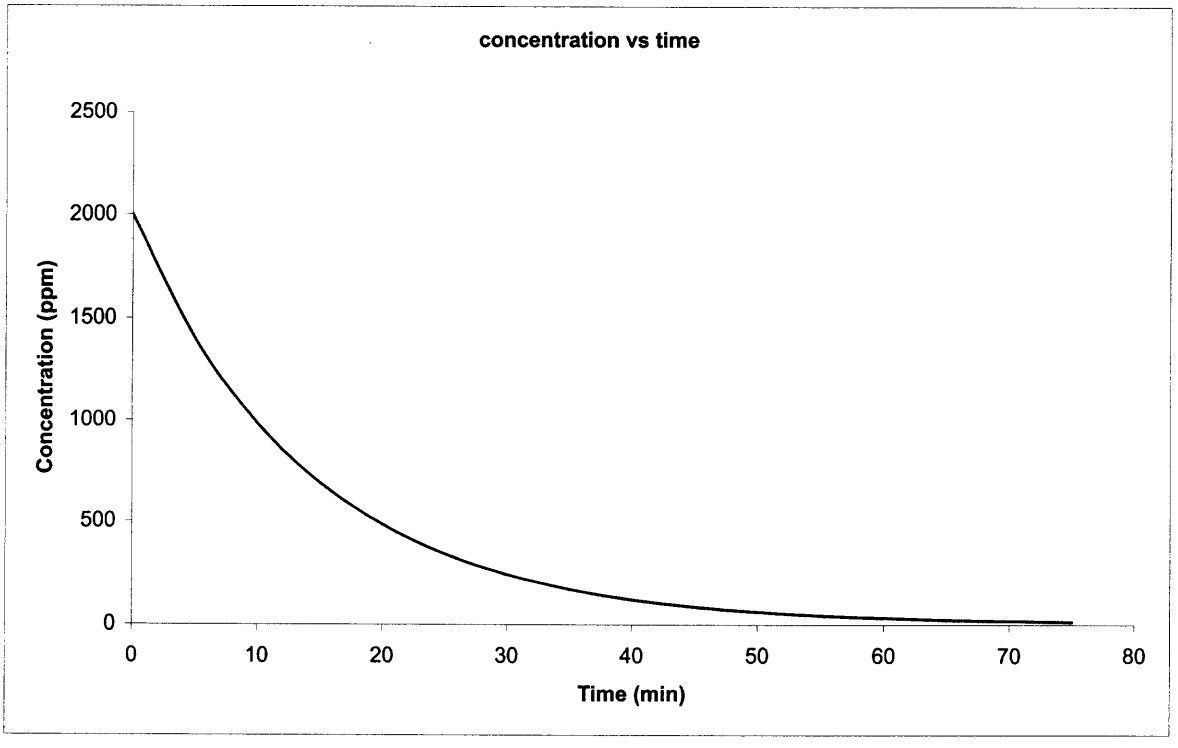


**Figure 9** Exponential Decrease in flask concentration from 2000 ppm to 4.4 ppm when 4.4 ppm toluene mixture is passed in a flask containing 200 ppm toluene at 13 ml/min.

nitrogen. This was done by closing valves 2 and 3 and positioning the two- way valve so that nitrogen would flow into the flask (Figure 6). Valve 1 was then opened and nitrogen allowed to flow through the flask for sufficient time to purge out the air and ensure that initially pure nitrogen was present in the flask. Valve 1 was then closed. In the case where the concentration in the flask was increasing from 0 ppm to 4.4 ppm, the two-way valve was positioned so that the gas would flow to the vent. Then valves two and three were opened and toluene was allowed to vent for a couple of minutes to remove the nitrogen containing high concentration of toluene and trapped between valves 2 and 3. The two-way valve was then positioned so that gas would flow through the flask. The nitrogen stream containing 4.4 ppm toluene was now flowing through the flask and the concentration in the flask increased exponentially to 4.4 ppm. The final concentration was reached after approximately 75 minutes.

In the case where the concentration in the flask was decreasing from 2000 ppm to 4.4 ppm, valves two and three were closed and the system was allowed to rest for a day. Then, after flushing the flask with nitrogen the two-way valve was positioned so that gas would flow into the flask.

When valve 1 was open and valve 2 was closed, the nitrogen would follow path A. At this point the two-way valve was positioned such that the gas would flow into the bulb. Thus, pure nitrogen would be flowing into the bulb and this was used to flush the flask before any run.

When valve 2 and valve 3 were open and valve 1 closed the nitrogen would flow through across the capillary and would entrain toluene in the process. Thus now nitrogen flowing into the flask would contain toluene.

When the system, with valve 2 and 3 closed, is allowed to stand for sufficient time the partial pressure of toluene in the nitrogen trapped between the two valves is the saturation pressure. Thus in order that a saturated stream of toluene flow in to the flask, the system was allowed to stand for a few hours and then valves 2 and 3 were opened, taking care that there was flow and the needle valve was open first.

Readings for the first set-up were taken by switching on the light at intervals of five minutes with one minute being allowed for the picoammeter reading to stabilize. Results for the experiments carried out with this set up are in section 4.1.

## 3.2 Experimental Apparatus II

The next set of experiments was carried out to measure differences in the photo resistance of the sensor for different concentrations of toluene. A batch system was designed for this purpose. It is as shown in Figure 10.

### 3.2.1 Apparatus

A new system was designed, as the earlier set up had a rubber stopper for the flask, which could both absorb and desorb toluene and play a role in the accuracy of the results. Also instead of exponential dilution the sensor could now be exposed to a prepared concentration of toluene. To eliminate the possibility of incomplete mixing in the dynamic system, a system where the sensor chamber could be evacuated and then filled with a gas of prepared concentration would be desirable. Thus, a new design

incorporating an air tight steel chamber was implemented. Another advantage was that the steel chamber did not allow ambient light to pass through.

In the second set-up the steel chamber had a glass window on top to let the light in. It had electrical connectors at the bottom to which the sensor was connected. The steel chamber can be seen in Figure B.4 (appendix B). The runs with this new set were carried out with broadband 450 nm filter. In the earlier set a 500 nm filter was used. The exit of the chamber was always closed. The inlet port was used to introduce gas into the chamber as well as to evacuate the chamber. This can be from the piping layout of Figure 10. A vacuum pump was attached to the outlet, and the valve arrangement facilitated isolating the supply gas cylinders so that the chamber could be evacuated.

The flow to the chamber could be switched between prepared gas mixture and nitrogen depending on whether the flask was being flushed or sensor being exposed to prepared gas mixture.

Since this was a batch process, the bubble flow meter was not attached at the exit of the chamber. At the inlet port an absolute pressure gauge was installed to measure vacuum and the pressure at which the experiment was carried out. In all cases the chamber was evacuated to 2.5 psi absolute and pressurized to 21 psi absolute with test gas mixture.

As opposed to the earlier case where the sensor was connected only to a picoammeter, in this case a recorder was added. The recorder gave graphs of current vs. time.

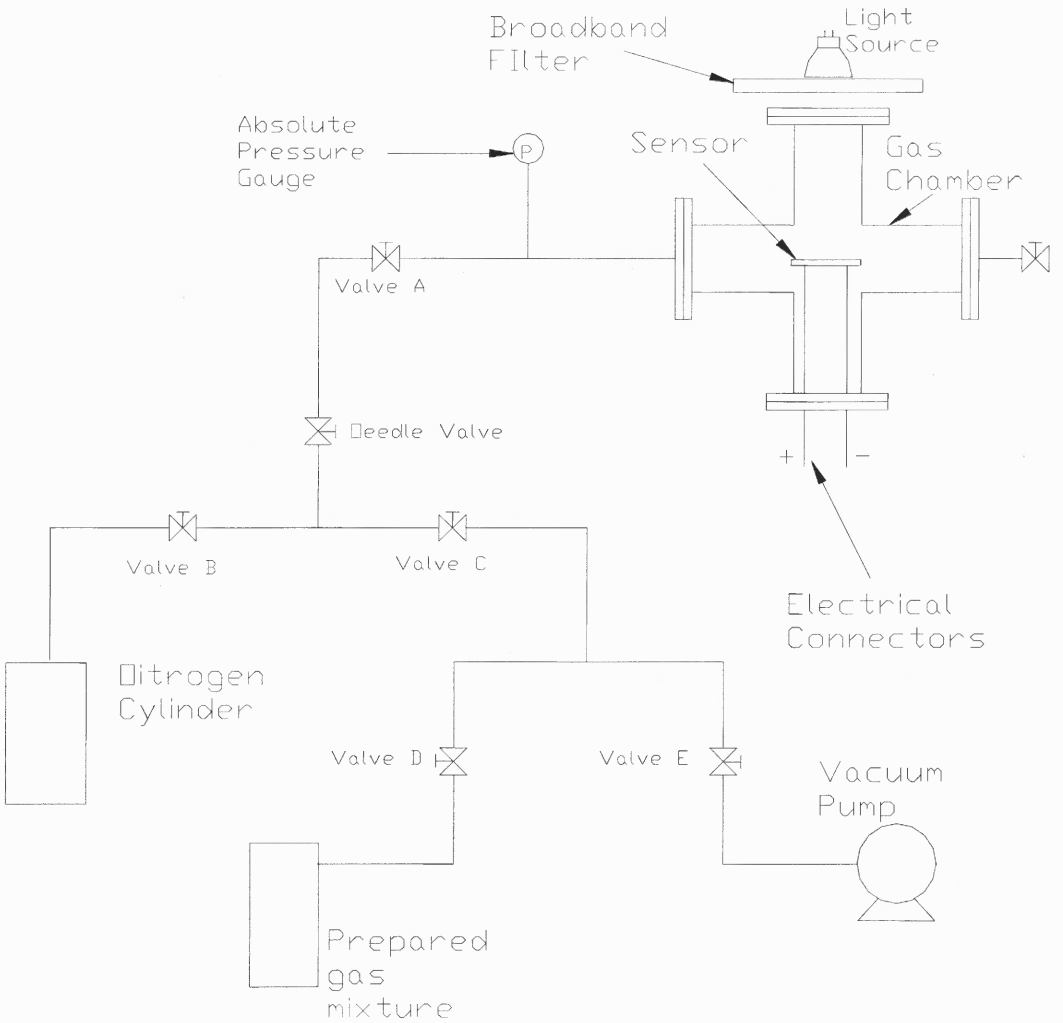


**Figure 10** Schematic of Experimental Set-Up II

In both the set-ups, to reduce electrical noise, the electricals of the set up were wrapped in copper net. The net itself was grounded and it acted as an antenna for electrical noise, which was reduced.

### 3.2.2. Procedure

In this case different approaches to take readings were tried to determine which approach gave the best results. In the first case, as in the earlier case the chamber was always flushed with nitrogen before any run. Valves B and D were closed, the needle valve, valve A and valve E were opened and vacuum pump run. This evacuated the flask. The flask was then flushed with nitrogen by first closing valves E and C and opening valves B, A and needle valve. In order to expose the sensor to prepared gas mixtures the gas mixture was introduced in to the chamber by first evacuating the chamber after flushing with nitrogen a couple of times. The chamber was pressurized to 21 psi absolute for all readings. While taking readings valve A was closed. Readings were taken by switching on the light at five minute intervals with sufficient time given for the readings on the recorder to stabilize. Results for the experiments carried out with this set-up are in section 4.2.

Careful observation revealed diffraction patterns of white light as well as filtered light falling on the sensor. The distance of the light from the filter was changed to produce a more even illumination. This can be seen in Figure B.1 (appendix B). This position of the light was fixed for all the following cases and the experiments were carried out with the light on continuously. Changing the position of the light with respect

to the sensor changed the intensity of light falling on the sensor, which in turn changed the current output for photoresistance of the sensor as compared to previous case.

In the next case, with the light on continuously, different concentrations of gases were fed to the chamber. Between different concentrations, the flask was not flushed and a 10 min time interval was allowed for each reading to stabilize. Then the chamber was pumped down to vacuum and the next concentration of gas let in.

The next case was similar to the previous case with one difference. In this case the chamber was flushed with nitrogen between runs. The chamber was flushed for a period of 10 min between runs.

In the next case, between runs with different concentrations, the chamber was flushed with nitrogen for the length of time required by the sensor to return to its initial value of photoresistance i.e. the value of photoresistance in vacuum. During each run, the sensor was exposed to toluene and as a result of that its photoresistance increased. When it was then flushed with nitrogen its photo resistance returned to its initial value. This ensured that the same initial conditions were being used to measure the change in the photoresistance.

## 3.3 Experimental Peripherals

### 3.3.1 Preparation of Gas Standards:

Three different concentrations of toluene in nitrogen were prepared- 50 ppm, 100 ppm and 200 ppm. Canisters were first evacuated and flushed several times with nitrogen, then while they were being filled with nitrogen to 50 psi, toluene was injected at the throat of

the canisters. The throat was heated to ensure that all the toluene injected had evaporated into the nitrogen. The canisters were allowed to sit for 24 hours before being used.

### 3.3.2 Coating the Sensor

A 1 mg /ml solution of Rhodamine B dye in Ethanol was prepared. The sensor was soaked in the solution for 15 min, removed and then left to dry for another 30 min. This procedure deposited a layer of the dye on the sensor.

### 3.3.3 Light used

The light source was a MR 15 Halogen manufactured by General Electric.

Specifications: 12 volts, 50 Watt, flood

### 3.3.4 Filter:

The filters were purchased from Edmund Industrial Optics. The filters used were Broadband 450 nm (model J46-149) and 500 nm (model J46-150), 11.8 mm diameter each. The specifications of filters is given below:

| | |
|---|---|
| Central Wavelength (CWL) Tolerance | = ± 15 nm |
| Full width-Half maximum (FWHM) | = 80nm ± 25nm |
| Peak Transmittance (min.) | = 60% |
| Thickness | = 9.65mm max. |

Thus the wavelength of incident light was between 410nm-490nm for the 450nm broadband filter and between 460 nm and 540nm for the 500nm broadband filter.

### 3.3.5 Toluene:

Toluene manufactured by J.T. Baker Chemical Company was used. It was 99% (by GC analysis) pure. The same toluene was used to prepare gas mixtures and in initial experiments for capillary diffusion.

### 3.3.6 Picoammeter

The picoammeter used was of the following make and type:

Keithley Current Amplifier: Model 427.

### 3.3.7 Recorder:

The recorder used was of the following make and type:

Kipp & Zonen: Model BD41

### 3.3.8 Chamber for Apparatus II:

Stainless steel cross-shaped chamber, 6 cm ID, with electrical pass-throughs on one end, a Pyrex window on the opposite end, and tube pass-throughs on the ends of the two other arms of the cross. This pressure/vacuum system has no polymeric seals in the gas stream and the internal chamber is all stainless steel or glass. The chamber was obtained from Kurt J. Lesker Co.

# CHAPTER 4

# RESULTS AND DISCUSSION

## 4.1 Experimental Apparatus I

The first step was to determine if the sensor was actually responding to light and to toluene. The set up described in section 3.1 and shown in figure 6 was used for this purpose.

When the sensor was exposed to light the resistance of the sensor dropped, that is the current flowing through the sensor increased for the same voltage being supplied. The resistance of the sensor with the light off is referred to as the dark resistance and with the light on is referred to as photoresistance. This change in resistance of the sensor will depend on a variety of factors such as the intensity of light incident on the sensor, the area of the sensor and the dye coating on the sensor.

If the light source is brought closer to the sensor then the light incident on the sensor increases. This results in the resistance of the sensor dropping down further. This is because if more light is incident on the sensor then more energy is available to excite dye molecules and they in turn can transfer more energy to the semiconductor layer, thus increasing the amount of energy available for photosensitized conductivity. Thus the resistance of the sensor drops as the light source is brought closer to the sensor.

Similarly, if the light source is kept at a fixed distance from the sensor and the amount of dye deposited on the sensor is varied by changing the time the sensor is soaked in the 1mg/ml ethanol solution, then, with more dye on the surface the change in

resistance with the light on will be more. This is again because of increase in energy for photosensitized conductivity. For the same amount of incident light more dye on the surface would mean that more energy would be absorbed and transferred to the semiconductor layer, thus decreasing the resistance.

Thus, for all the experiments the sensor was soaked in the dye solution for a period of 15 minutes. Also the light was maintained at fixed distance in each set of experiments. In the case of the second set of experiments the light was further away from the sensor as compared to the first set because of the size of the gas chamber and to avoid diffraction effects of the filter.

### 4.1.1 Flask Concentration Decreasing Exponentially:

Experiments carried out with the concentration in the flask decreasing exponentially from 2000 ppm to 4.4 ppm, showed that the dark resistance of the sensor decreased with time. This can be seen in Figure 11. Readings were taken at intervals of five minutes and one minute was allowed to stabilize the reading i.e. the light was switched on after every five minutes and the current reading was taken one minute after the light was switched on.

A graph of photoresistance of the sensor as a function of concentration, Figure 12, showed that the photoresistance decreased with concentration, and the trend is similar to the decrease in dark resistance of the sensor. In this case, the photo resistance of the sensor should drop rapidly initially, due to the sensor being exposed to a high concentration of toluene, and then it should increase as the concentration of toluene in the flask drops from 2000 ppm to 4.4 ppm. But as can be seen from the graph the photo resistance drops continuously.

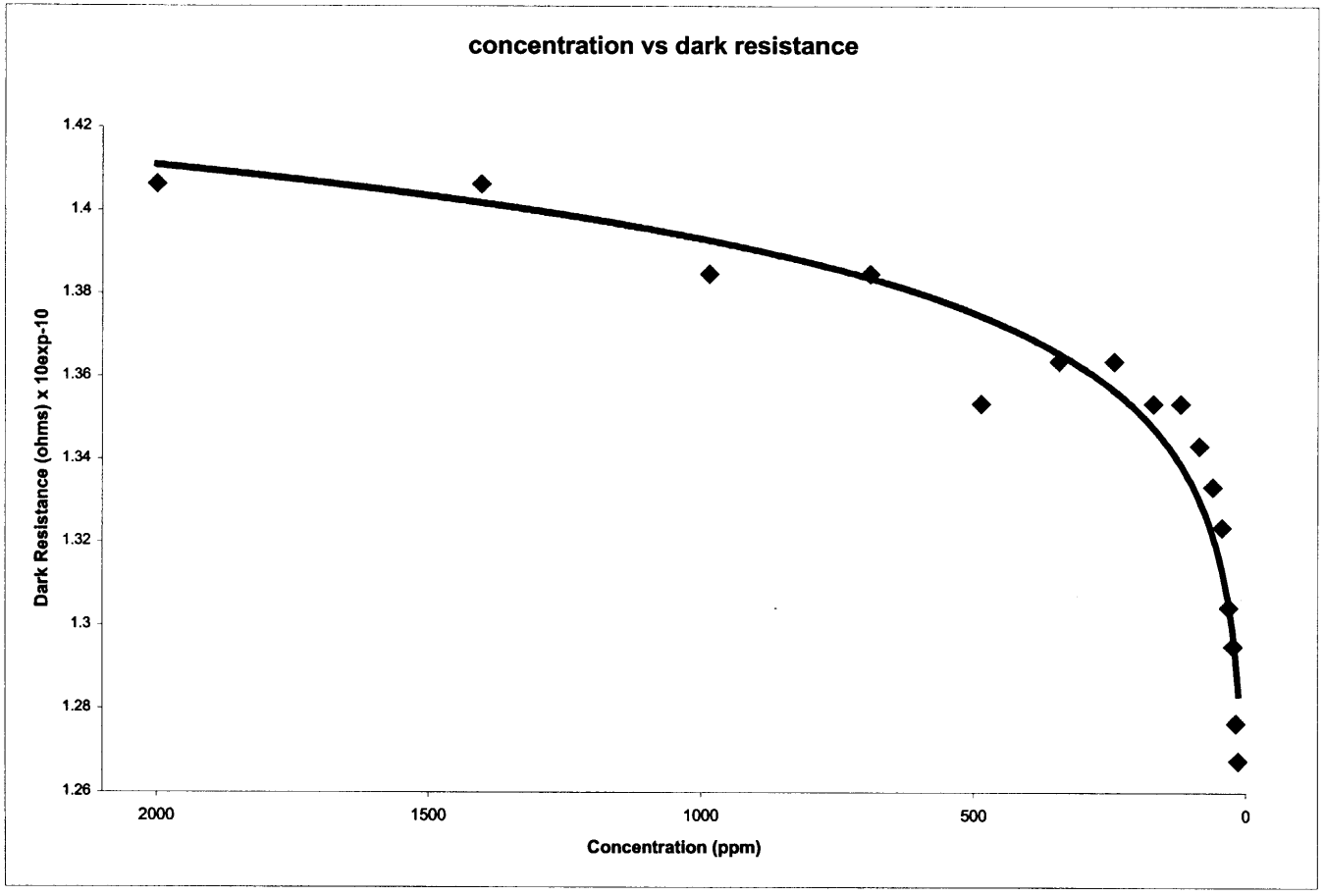


**Figure 11** Change in Dark Resistance as a function of Concentration. The curve represents the best fitting line for the data obtained.

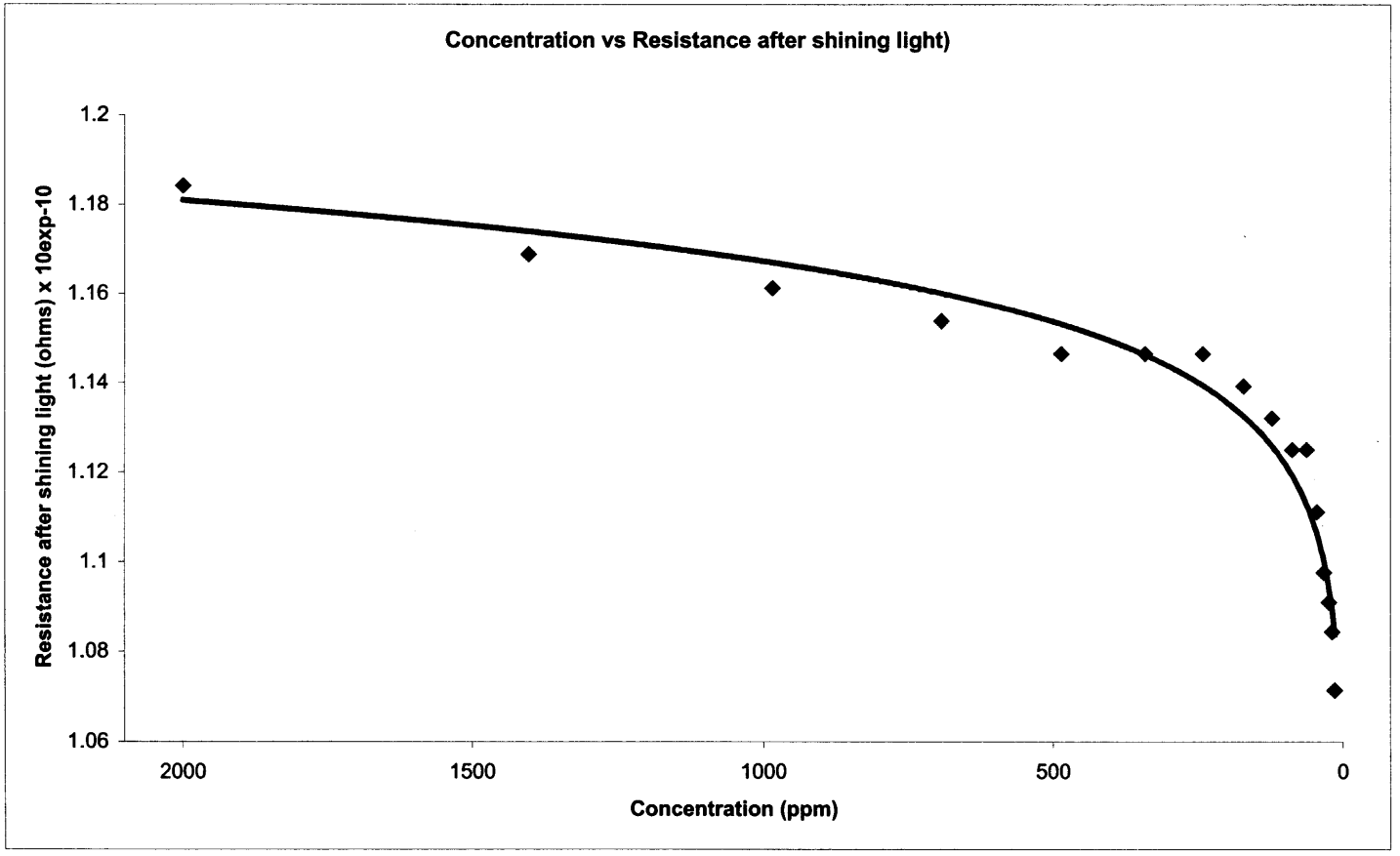


**Figure 12** Photoresistance as a function of concentration. The curve represents the best fitting line for the data obtained.

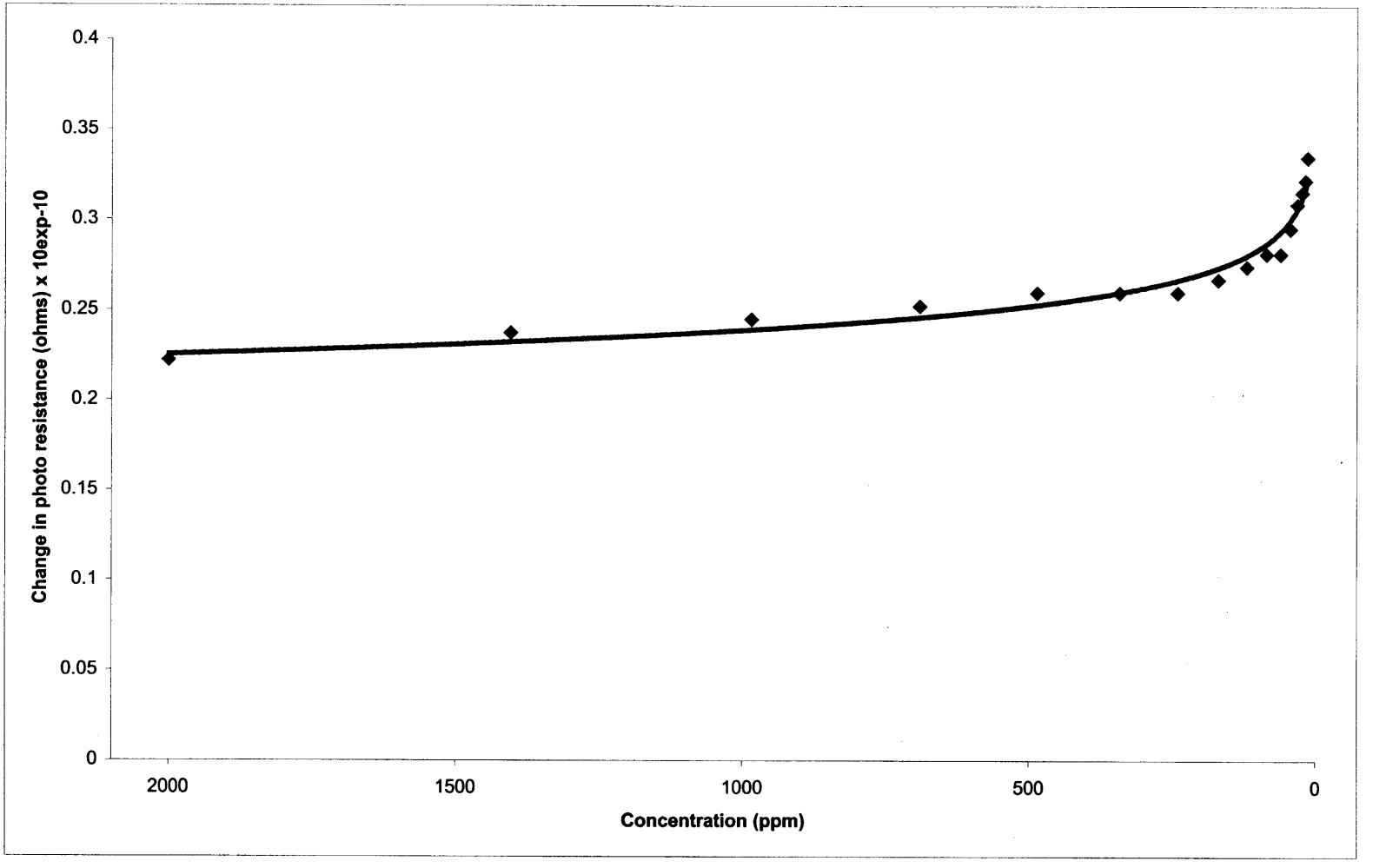


**Figure 13** Change in Resistance i.e. Photoresistance - Dark Resistance (at time t=0) as a function of concentration. The curve represents the best fitting line for the data obtained.

Figure 13 shows the change in resistance i.e. difference between photoresistance and dark resistance (measured with no toluene in the flask) as a function of concentration. The change in resistance decreases as function of concentration. The difference in dark resistance and photoresistance of the sensor should decrease as concentration of toluene in the flask increases. But in this case the concentration is decreasing and so the graph should show an increasing trend.

The sensor behavior for this case can be attributed to two reasons: either the response time of the sensor is too high and thus it takes a long time for the sensor and the surrounding gas to reach equilibrium, or the gas in the flask is not mixed properly and toluene diffuses slowly through the gas onto the sensor surface. Also since the sensor was initially exposed to a high concentration of toluene it is possible that the sensor surface was saturated by toluene and the toluene was not desorbing with decrease in surrounding concentration. But in either case the sensor does respond to the presence of toluene.

### 4.1.2 Exponential Increase in Flask Concentration:

Next the concentration in the flask was increased from 0 ppm to 4.4 ppm and readings at every 5-minute interval were taken in the same way as done previously. A graph of resistance vs. time, Figure 14, for the sensor shows that the sensor photoresistance falls continuously as the concentration increases to 4.4 ppm. The concentration in the flask increases to 4.4 ppm in about 75 min. After 75 min the flow was switched off and the photoresistance of the sensor was monitored. The photoresistance as a function of time, under conditions of constant concentration of 4.4 ppm in the flask, for a period of 30 min is plotted in Figure 15.

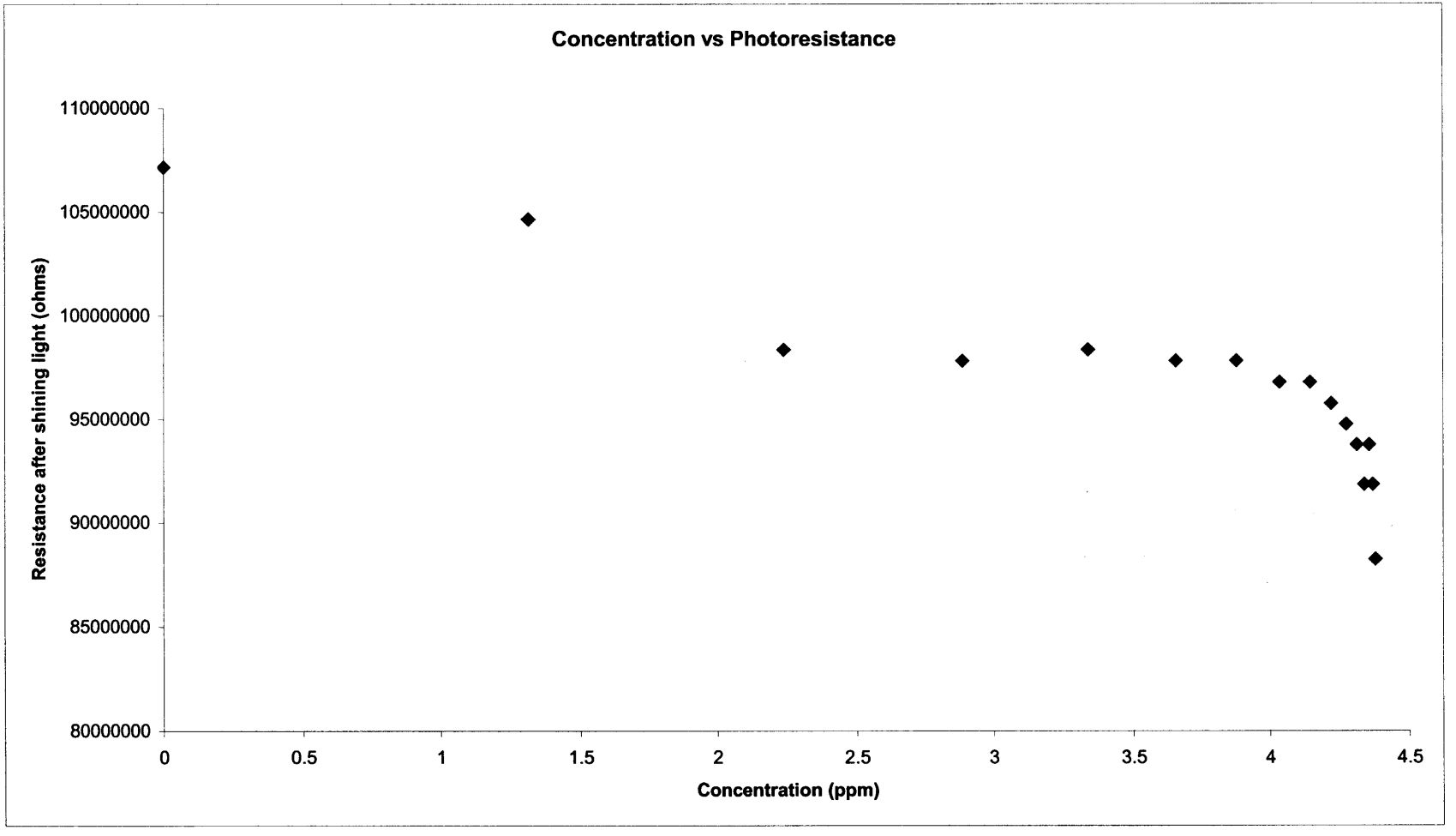


**Figure 14** Photoresistance as a function of Concentration for the concentration in the flask increasing exponentially from 0 ppm to 4.4 ppm.

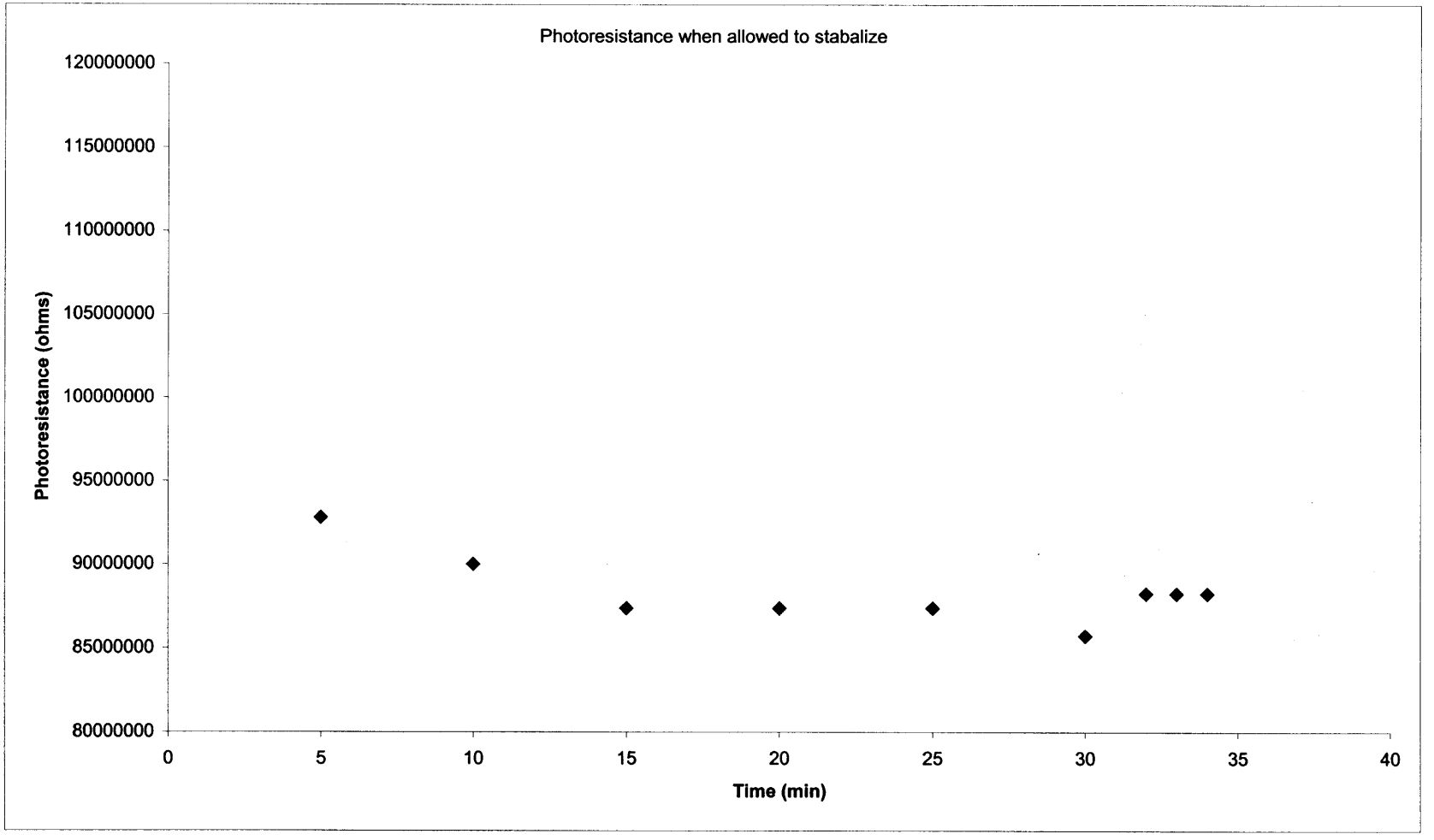


**Figure 15** Photoresistance as a function of time at the end of 80 min and constant concentration of toluene in the flask.

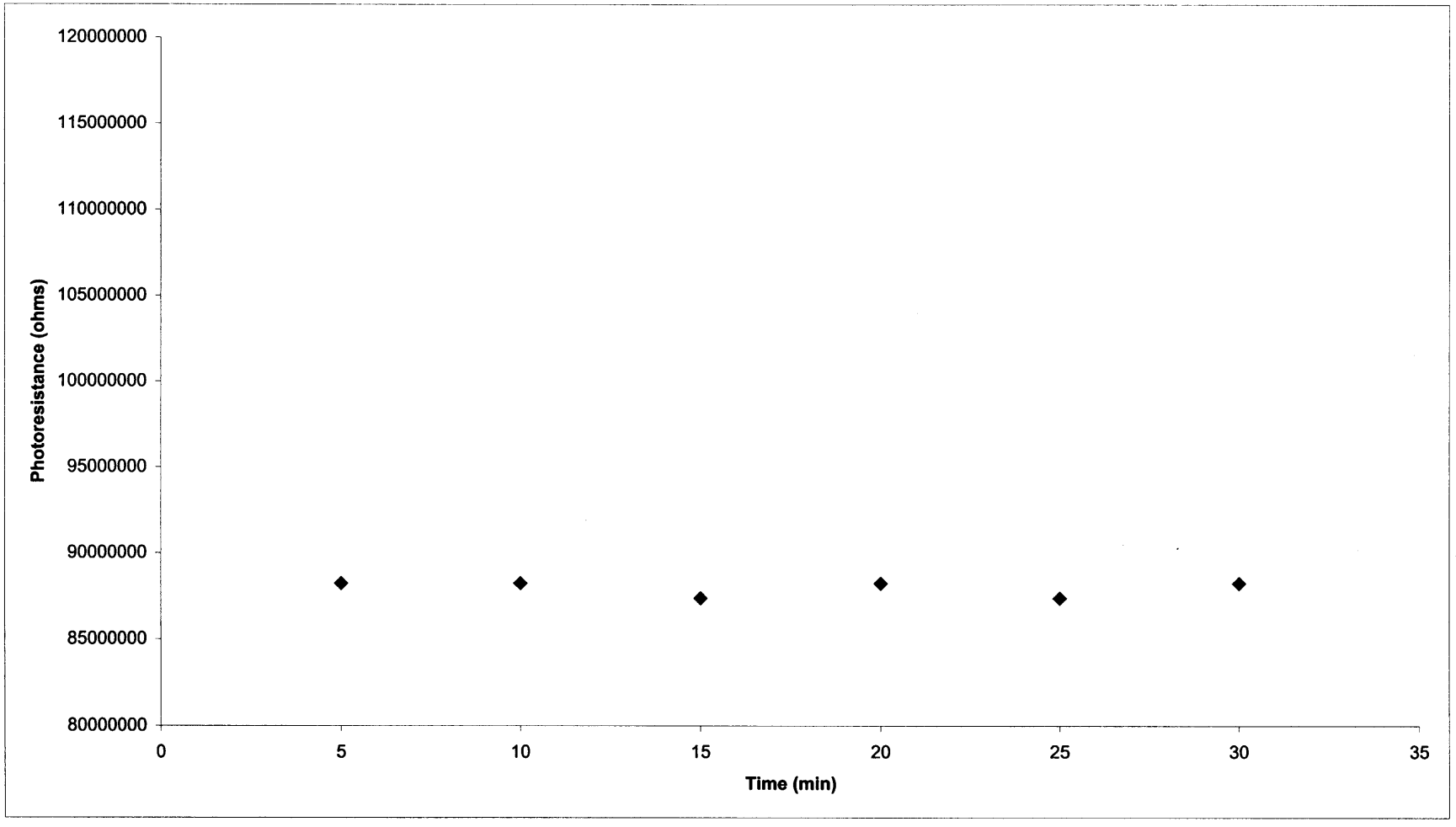


**Figure 16** Photoresistance as a function of time for purge after sensor was allowed to stabilize for 35 min.

As can be seen from the graph of figure 15, the photoresistance of the sensor does not change significantly for a period of 35 min under conditions of constant concentration. Initially, for the first 10 minutes, there is a slight drop in photoressitance that is due to the sensor and toluene reaching equilibrium. At the end of 35 minutes, a pure nitrogen stream at the same flow rate of 13 ml/min was introduced into the flask. Thus, now the concentration of toluene in the flask was again deceasing from 4.4. ppm and tending to zero. The response for a period of 30 min was noted and from Figure 17 shows that the sensor photoresistance did not change significantly.

This indicates that, for low concentrations mixing within the flask and equilibrium between the sensor and were not of concern for low toluene concentrations in the flask. Also, the fact that the sensor was not responding to a decrease in concentration indicates that the rate of desorption of absorbed toluene from the surface of the sensor was very low. Also, if the flask was flushed with nitrogen and the sensor exposed to toluene again then it did respond to increasing toluene concentration.

In order to eliminate the possibility of improper mixing a magnetic pellet and a stirrer were incorporated in the design. However, the magnetic stirrer caused a lot of electrical noise and was discarded.

The experiments described above indicate that that the sensor was responding to toluene as desired. The next step was to study the sensor response to different toluene concentrations. A different experimental arrangement was used for the purpose.

## 4.2 Experimental Apparatus II

The earlier experiments were not free of errors as the rubber stopper being used to seal the flask was capable of absorbing and desorbing toluene and thus could be a source of error. Also to eliminate the possibility of improper mixing, evacuating the flask and exposing the sensor to the desired toluene concentration, a system where the sensor chamber could be evacuated and then filled with a gas of prepared concentration would be desirable. Thus a new design incorporating a air tight steel chamber was implemented.

The purpose of the new set-up was to demonstrate that the sensor was capable of distinguishing between different concentrations of toluene. Four different concentrations of gases were prepared – 20 ppm, 50 ppm, 100 ppm and 200 ppm. The sensor was exposed to these different concentrations and the change in resistance of the sensor was measured as a function of time.

In the first case, readings were taken at regular intervals of three minutes, and the light was left for 5 min for each reading. The sensor response is as represented in the graph in Figure 17. As the concentration of the analyte on the sensor surface increases, the photoexcited dye molecules will transfer more of their energy to the analyte and less energy will be available for photoconductivity. Thus, the change in photo resistance of the sensor when exposed to 50 ppm should be higher than that for a higher concentration which is as obtained in the results. As can be seen from the results, the best sensitivity is at lower concentrations. The results of Figure 17, were reproducible and were repeated two times and the change in photoresistance was found to be similar to the changes shown in Figure 17.

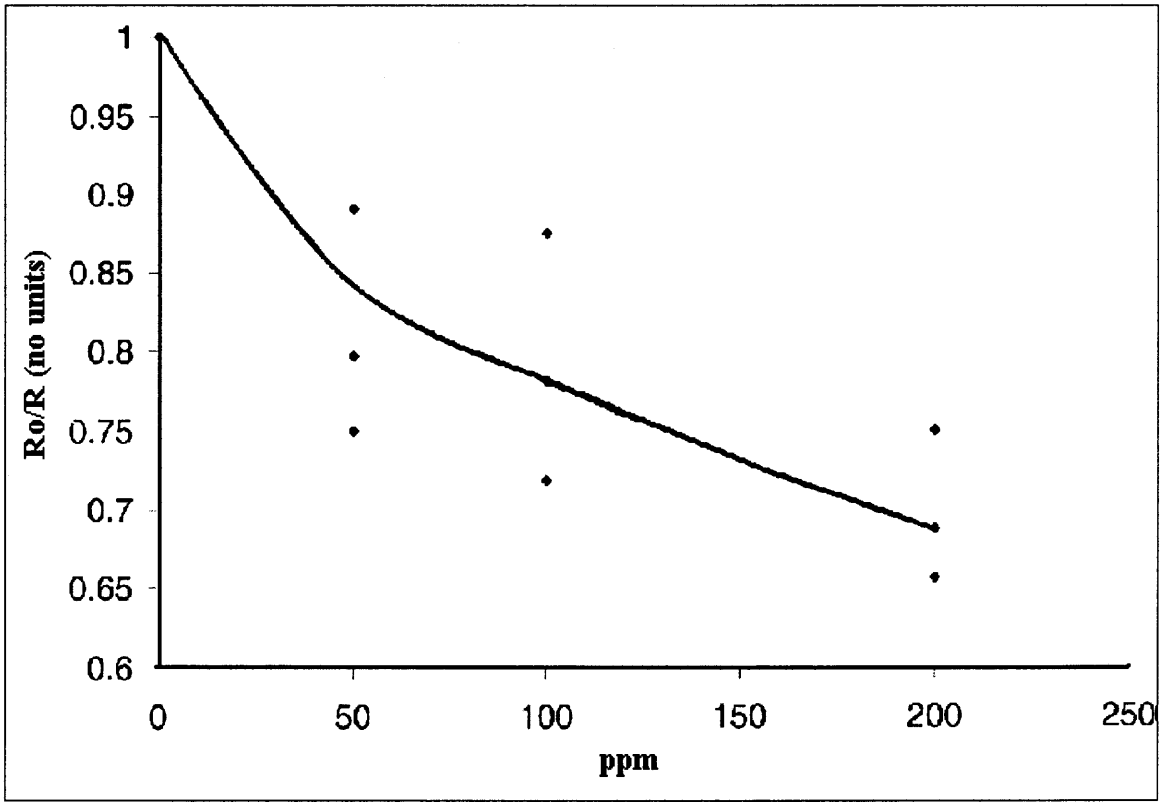


**Figure 17** Response to toluene (with light turned on and off at regular intervals): The resistance is normalized to that found with pure nitrogen or with vacuum (which give the same response when the sensor is adequately reconditioned between changes of toluene concentration). The line indicates the average change in photoresistance for a particular concentration.

For the remaining experiments, as described in section 3.2.2, the light was on continuously. In one set, the experiments were carried out with no nitrogen flushing in between runs and different concentrations of toluene were introduced in the chamber. The chamber was evacuated after each run. It was observed that the resistance of the photoresistance of the sensor dropped to the same value in each case i.e. for 25 ppm, 50 ppm, 100 ppm and 200 ppm. This is because, with repeated toluene exposures and no nitrogen flushing, the surface of the sensor was saturated with toluene. Thus it was decided that flushing with nitrogen was essential for desorption of toluene from sensor surface.

In the next set of runs the chamber was flushed with nitrogen, between successive runs with increasing concentrations of 25 ppm, 50 ppm, 100 ppm and 200 ppm. A fixed time interval of ten minutes was decided as the time to flush the flask. However in this case too it was observed that different concentrations did not result in any significant changes between successive readings. This could again be attributed to insufficient flushing with nitrogen and the sensor surface getting saturated with toluene. Then the time for flushing with nitrogen was increased to the time taken by the sensor to return to its initial photoresistance value i.e. under conditions of vacuum. Thus for each reading the sensor photoresistance was at the same initial value. Even in this case the sensor did not respond as expected and showed no significant difference between different concentrations. Inspection of the nitrogen line revealed a leak in the nitrogen supply line, a source of oxygen to enter the system.

This leak was rectified and the experiment repeated as in the previous case, where the time for flushing with nitrogen was increased to the time taken by the sensor to return

to its initial photoresistance value. The sensor was exposed to concentrations of 2.6 ppm, 5.3 ppm, 8 ppm, 10.7 ppm, 13.3 ppm, 20 ppm, 50 ppm and 100 ppm. The lower concentrations i.e. less than 20 ppm, were prepared by diluting the 20 ppm toluene mixture with nitrogen using an accurate pressure gauge. In this case the sensor response was as expected is shown in Figure 18. The results are plotted as ratio of photoresistance for that reading and the photoresistance in vacuum. As can be seen the photoresistance decreases as the concentration of toluene increases. In this set of readings it took on an average one hour for the chamber to be cleaned completely free of toluene. This was confirmed by introducing nitrogen and monitoring the system for changes in sensor photoresistance.

As can be seen from the graph the sensor shows high changes in its photoresistance for lower concentrations. Also for this set of run the sensor was exposed to light for extended periods and that did not affect the readings. Thus extended exposure to light does not have a negative effect on the sensor.

In this set of experiments the rate of change of photoresistance of the sensor to different toluene concentrations was also monitored and it was observed that the rate of decrease in photoresistance was higher for higher concentrations. The graph of Figure 19 shows that for a fixed period of ten minutes (in this time period the photoresistance decreases almost linearly with time) the sensor photoresistance drops to a lower value for higher concentrations e.g. 100 ppm as compared to that for a lower concentration e.g. 20 ppm. The rate of drop of photoresistance could also be used as an indication of the concentration of toluene in the gas in contact with the sensor.

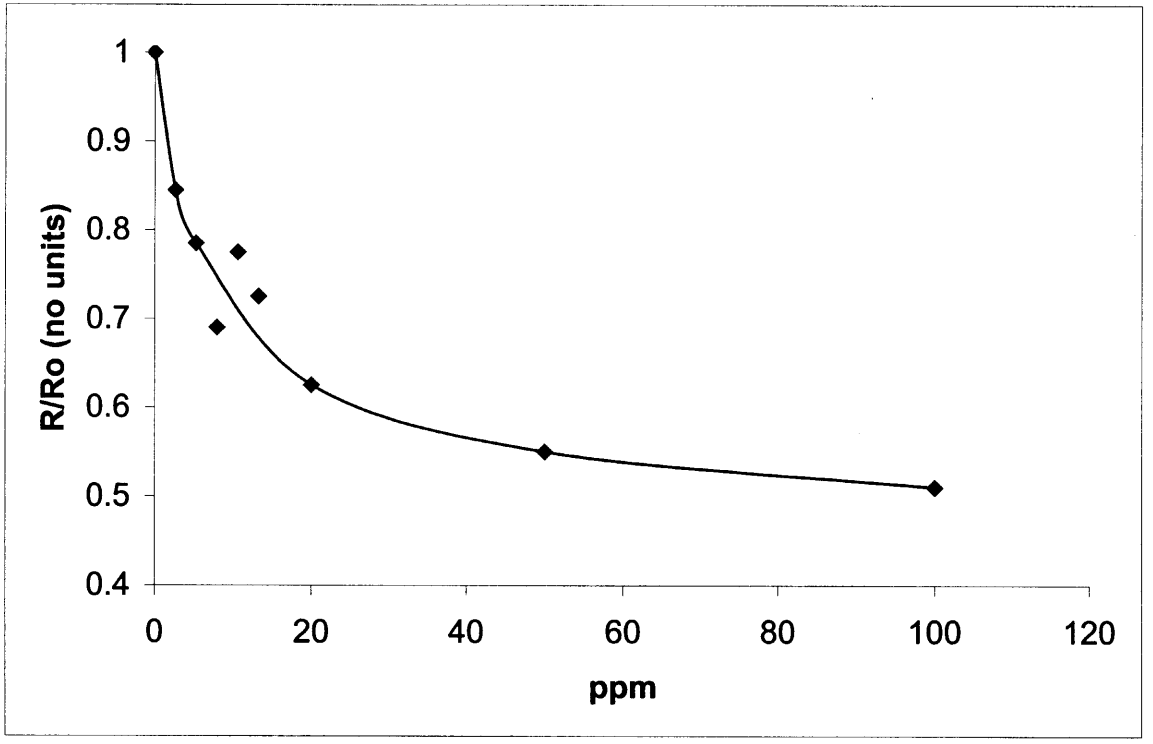


**Figure 18** Response to toluene with adequate time to purge the chamber and light continuously on: The resistance is normalized to that found with pure nitrogen or with vacuum (which give the same response when the sensor is adequately reconditioned between changes of toluene concentration). The line indicates the best fit.

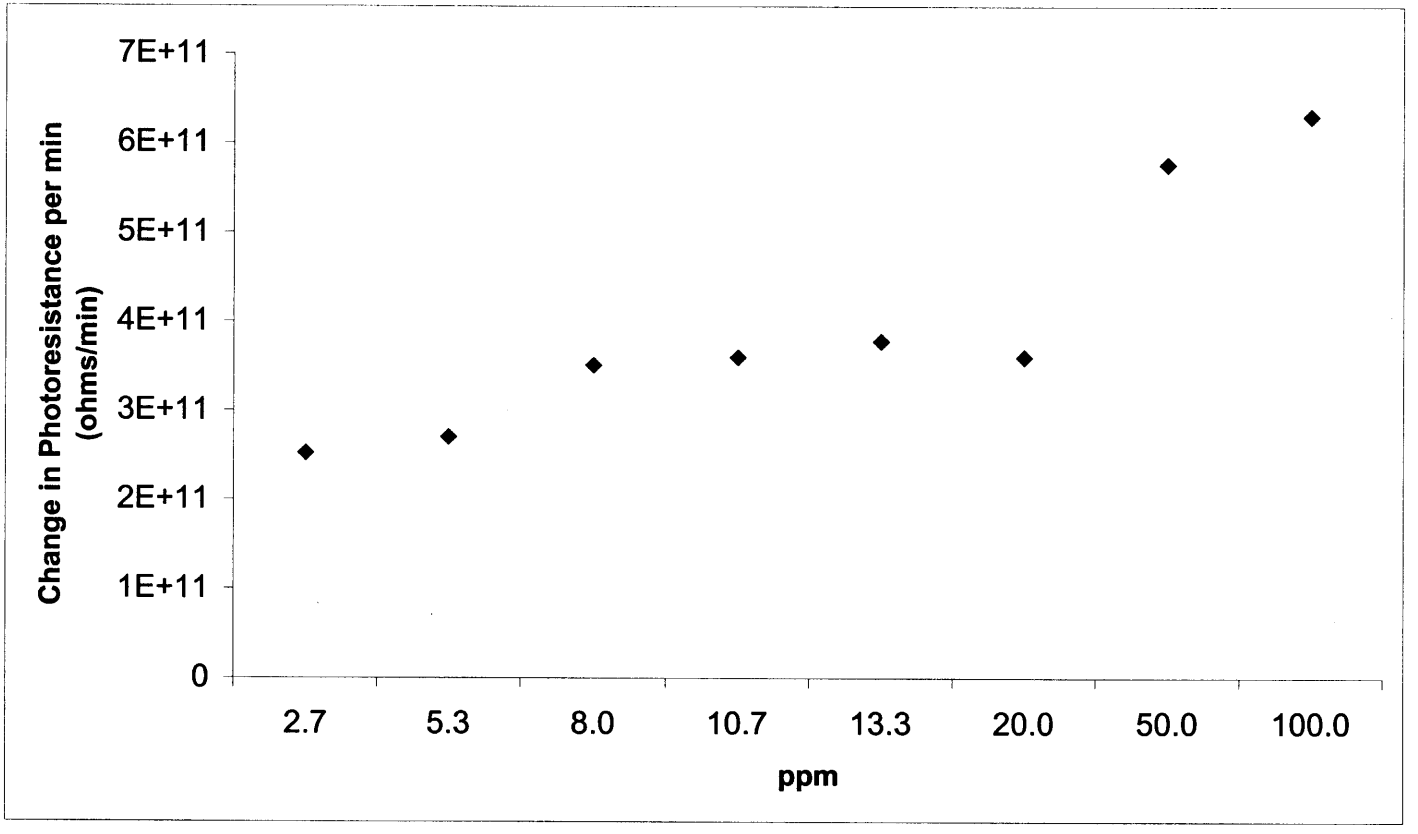


**Figure 19** Graph of change in resistance per minute for different toluene concentrations. The rate of change of photoresistance is maximum for 100 ppm and least for 2.7 ppm.

### 4.3 Future Work

We have successfully demonstrated that the sensor is sensitive to light and it responds to different concentrations of toluene in nitrogen. The gas mixtures tested were free of water vapor and oxygen. The change in its photoresistance is higher for lower concentrations. The sensor still has to be tested for response to other organic vapors such as olefins and their mixtures. Also future tests will have to be done in the presence of water vapor and oxygen in the gas stream as these could have an effect on the selectivity and response of the sensor.

The sensor response on the recorder has a lot of noise and that can be either intrinsic to the sensor or it could be a result of fluctuations in light intensity. A comparison of the results obtained in this thesis with a more stable, battery powered light source should give an indication of the source of the noise.

The rate of desorption of toluene from the sensor is very slow as can be seen from the time it takes for the photoresistance of the sensor to return to its value in vacuum which is approximately one hour. For faster time between readings the sensors will have to have better desorption characteristics. The rate of desorption increases with temperature. Hence one way to achieve faster desorption is to build a sensor chip with a heater strips on the bottom of the glass substrate.

# APPENDIX A

# DATA FROM EXPERIMENTS

**Table I**

| Time (min) | Concentration (ppm) | Dark Resistance R1 (ohms) | Resistance After shining light R2 (ohms) | Change in resistance (R1 - R2) (ohms) | Change in Resistance (1.41E+10 - R2) (ohms) |
|---|---|---|---|---|---|
| 0 | 2000.00 | 1.41E+10 | 1.18E+10 | 2.22E+09 | 2.22E+09 |
| 5 | 1403.15 | 1.41E+10 | 1.17E+10 | 2.37E+09 | 2.37E+09 |
| 10 | 984.81 | 1.38E+10 | 1.16E+10 | 2.23E+09 | 2.45E+09 |
| 15 | 691.58 | 1.38E+10 | 1.15E+10 | 2.31E+09 | 2.52E+09 |
| 20 | 486.06 | 1.35E+10 | 1.15E+10 | 2.07E+09 | 2.60E+09 |
| 25 | 342.00 | 1.36E+10 | 1.15E+10 | 2.17E+09 | 2.60E+09 |
| 30 | 241.03 | 1.36E+10 | 1.15E+10 | 2.17E+09 | 2.60E+09 |
| 35 | 170.26 | 1.35E+10 | 1.14E+10 | 2.14E+09 | 2.67E+09 |
| 40 | 120.65 | 1.35E+10 | 1.13E+10 | 2.21E+09 | 2.74E+09 |
| 45 | 85.88 | 1.34E+10 | 1.13E+10 | 2.18E+09 | 2.81E+09 |
| 50 | 61.51 | 1.33E+10 | 1.13E+10 | 2.08E+09 | 2.81E+09 |
| 55 | 44.43 | 1.32E+10 | 1.11E+10 | 2.12E+09 | 2.95E+09 |
| 60 | 32.46 | 1.30E+10 | 1.10E+10 | 2.07E+09 | 3.09E+09 |
| 65 | 24.07 | 1.29E+10 | 1.09E+10 | 2.04E+09 | 3.15E+09 |
| 70 | 18.18 | 1.28E+10 | 1.08E+10 | 1.92E+09 | 3.22E+09 |
| 75 | 14.06 | 1.27E+10 | 1.07E+10 | 1.96E+09 | 3.35E+09 |

Concentration in the flask in decreasing exponentially from 2000 ppm to 4.4 ppm (figures 12,13,14).

**Table II**

| Time (min) | Concentration (ppm) | Dark Resistance R1 (ohms) | Resistance after shining light R2 (ohms) | Change in resistance (R1 - R2) (ohms) | Current with light off (amps) | Current with light on (amps) |
|---|---|---|---|---|---|---|
| 0 | 0 | 9.00E+09 | 1.07E+08 | 8.89E+09 | 1.00E-09 | 8.40E-08 |
| 5 | 1.32 | 9.00E+09 | 1.05E+08 | 8.90E+09 | 1.00E-09 | 8.60E-08 |
| 10 | 2.24 | 9.00E+09 | 9.84E+07 | 8.90E+09 | 1.00E-09 | 9.15E-08 |
| 15 | 2.88 | 9.00E+09 | 9.78E+07 | 8.90E+09 | 1.00E-09 | 9.20E-08 |
| 20 | 3.34 | 9.00E+09 | 9.84E+07 | 8.90E+09 | 1.00E-09 | 9.15E-08 |
| 25 | 3.66 | 9.00E+09 | 9.78E+07 | 8.90E+09 | 1.00E-09 | 9.20E-08 |
| 30 | 3.88 | 9.00E+09 | 9.78E+07 | 8.90E+09 | 1.00E-09 | 9.20E-08 |
| 35 | 4.03 | 9.00E+09 | 9.68E+07 | 8.90E+09 | 1.00E-09 | 9.30E-08 |
| 40 | 4.14 | 9.00E+09 | 9.68E+07 | 8.90E+09 | 1.00E-09 | 9.30E-08 |
| 45 | 4.22 | 9.00E+09 | 9.57E+07 | 8.90E+09 | 1.00E-09 | 9.40E-08 |
| 50 | 4.27 | 9.00E+09 | 9.47E+07 | 8.91E+09 | 1.00E-09 | 9.50E-08 |
| 55 | 4.31 | 9.00E+09 | 9.38E+07 | 8.91E+09 | 1.00E-09 | 9.60E-08 |
| 60 | 4.34 | 9.00E+09 | 9.18E+07 | 8.91E+09 | 1.00E-09 | 9.80E-08 |
| 65 | 4.36 | 9.00E+09 | 9.38E+07 | 8.91E+09 | 1.00E-09 | 9.60E-08 |
| 70 | 4.37 | 9.00E+09 | 9.18E+07 | 8.91E+09 | 1.00E-09 | 9.80E-08 |
| 75 | 4.38 | 9.00E+09 | 8.82E+07 | 8.91E+09 | 1.00E-09 | 1.02E-07 |
| 80 | 4.39 | 9.00E+09 | 9.00E+07 | 8.91E+09 | 1.00E-09 | 1.00E-07 |

Exponential increase in flask concentration from 0 ppm to 4.4 ppm (figure 15).

**Table III**

| Time (min) | Concentration (ppm) | Dark Resistance R1 (ohms) | Resistance after shining light R2 (ohms) | Change in resistance (R1 - R2) (ohms) | Current with light off | Current with light on |
|---|---|---|---|---|---|---|
| 5 | 4.4 | 9.00E+09 | 9.28E+07 | 8.91E+09 | 1.00E-09 | 9.70E-08 |
| 10 | 4.4 | 9.00E+09 | 9.00E+07 | 8.91E+09 | 1.00E-09 | 1.00E-07 |
| 15 | 4.4 | 9.00E+09 | 8.74E+07 | 8.91E+09 | 1.00E-09 | 1.03E-07 |
| 20 | 4.4 | 9.00E+09 | 8.74E+07 | 8.91E+09 | 1.00E-09 | 1.03E-07 |
| 25 | 4.4 | 9.00E+09 | 8.74E+07 | 8.91E+09 | 1.00E-09 | 1.03E-07 |
| 30 | 4.4 | 9.00E+09 | 8.57E+07 | 8.91E+09 | 1.00E-09 | 1.05E-07 |
| 32 | 4.4 | 9.00E+09 | 8.82E+07 | 8.91E+09 | 1.00E-09 | 1.02E-07 |
| 33 | 4.4 | 9.00E+09 | 8.82E+07 | 8.91E+09 | 1.00E-09 | 1.02E-07 |
| 34 | 4.4 | 9.00E+09 | 8.82E+07 | 8.91E+09 | 1.00E-09 | 1.02E-07 |

Initially the concentration in the flask was increasing exponentially from 0 ppm to 4.4 ppm. When the flask concentration reached 4.4 ppm the flow to the flask was stopped. These readings were for the sensor when there was no gas flowing into the flask, the toluene concentration in the flask was 4.4 ppm and the readings were taken for a period of 34 min (figure 16).

**Table IV**

| Time (min) | Concentration (ppm) | Dark Resistance R1 (ohms) | Resistance after shining light R2 (ohms) | Change in resistance (R1 - R2) (ohms) | Current with light off | Current with light on |
|---|---|---|---|---|---|---|
| 5 | 3.08 | 9.00E+09 | 8.82E+07 | 8.91E+09 | 1.00E-09 | 1.02E-07 |
| 10 | 2.16 | 9.00E+09 | 8.82E+07 | 8.91E+09 | 1.00E-09 | 1.02E-07 |
| 15 | 1.52 | 9.00E+09 | 8.74E+07 | 8.91E+09 | 1.00E-09 | 1.03E-07 |
| 20 | 1.06 | 9.00E+09 | 8.82E+07 | 8.91E+09 | 1.00E-09 | 1.02E-07 |
| 25 | 0.74 | 9.00E+09 | 8.74E+07 | 8.91E+09 | 1.00E-09 | 1.03E-07 |
| 30 | 0.52 | 9.00E+09 | 8.82E+07 | 8.91E+09 | 1.00E-09 | 1.02E-07 |

Photoresistance of the sensor when the flask with 4.4 ppm toluene was purged after allowing it to stabilize for 34 min (figure 17). The concentration in the flask was dropping with time as it was being purged with nitrogen.

**Table V**

| Reading | Change in Resistance(light on as compared to light off) | | | |
|---|---|---|---|---|
| | **Vacuum 0** | **50** | **100** | **200** |
| 1 | 1.44E+12 | 1.08E+12 | 1.035E+12 | 9.45E+11 |
| 2 | 1.44E+12 | 1.1475E+12 | 1.125E+12 | 1.08E+12 |
| 3 | 1.305E+12 | 1.305E+12 | 1.1475E+12 | 1.035E+12 |
| 4 | 1.44E+12 | 1.2825E+12 | 1.26E+12 | 9.9E+11 |
| 5 | 1.3275E+12 | 1.26E+12 | 1.2375E+12 | |
| **Average** | 1.3905E+12 | 1.215E+12 | 1.161E+12 | 1.0125E+12 |
| **% Standard Dev.** | 4.9 | 8 | 7.8 | 5.7 |

Photoresistance of the sensor at different concentrations of toluene (figure 18).

**Table VI**

| ppm | Ratio of Photoresistance at particular ppm to Photoresistance at vacuum |
|---|---|
| 0.00 | 1.00 |
| 2.67 | 0.85 |
| 5.33 | 0.79 |
| 8.00 | 0.69 |
| 10.67 | 0.78 |
| 13.33 | 0.73 |
| 20.00 | 0.63 |
| 50.00 | 0.55 |
| 100.00 | 0.51 |

Ratio of photoresistance of the sensor at a particular toluene concentration to photo resistance at vacuum is calculated based on the recorder output as measured in distance (figure 19).

**Table VII**

| ppm | Change in resistance in 10 min |
|---|---|
| 2.7 | 2.52E+11 |
| 5.3 | 2.7E+11 |
| 8.0 | 3.51E+11 |
| 10.7 | 3.6E+11 |
| 13.3 | 3.78E+11 |
| 20.0 | 3.6E+11 |
| 50.0 | 5.76E+11 |
| 100.0 | 6.3E+11 |

The change in photoresistance of the sensor for a period of 10 minutes based on the recorder graph. A change of 1 cm on the recorder corresponds to a change of $9x10^{11}$ ohms (figure 20).

# APPENDIX B

# PICTURES

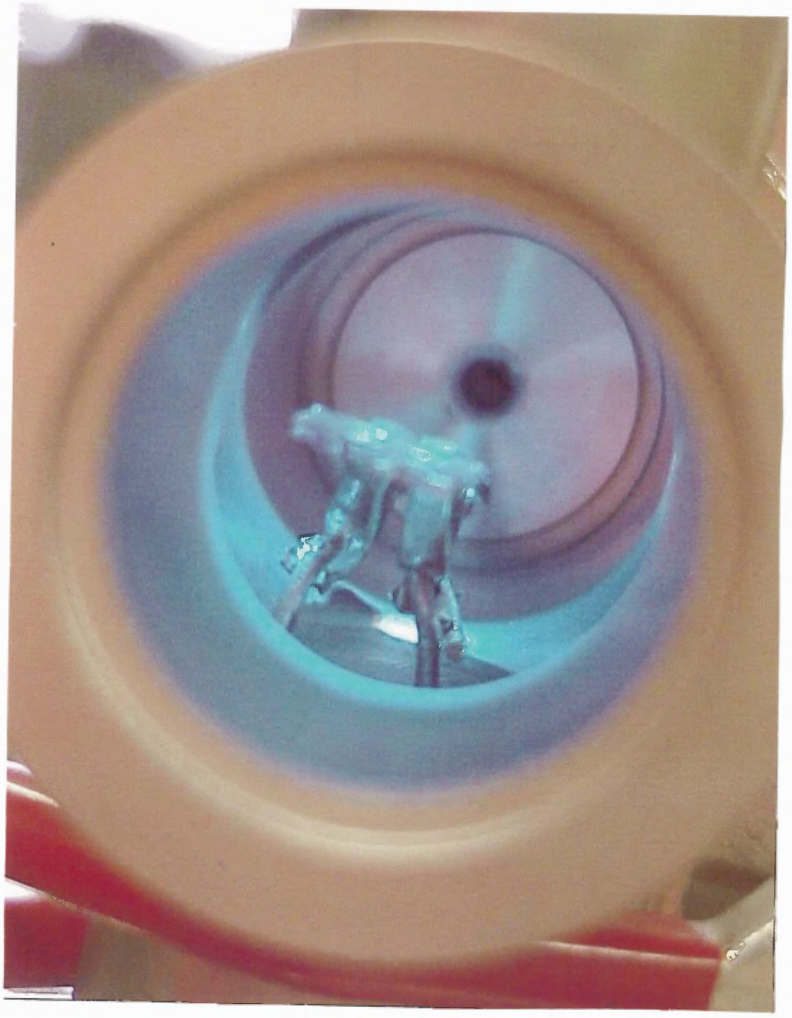

**Figure B.1** View of Sensor, with the light on, inside the steel chamber.

**Figure B.2** View of light incident on the sensor.

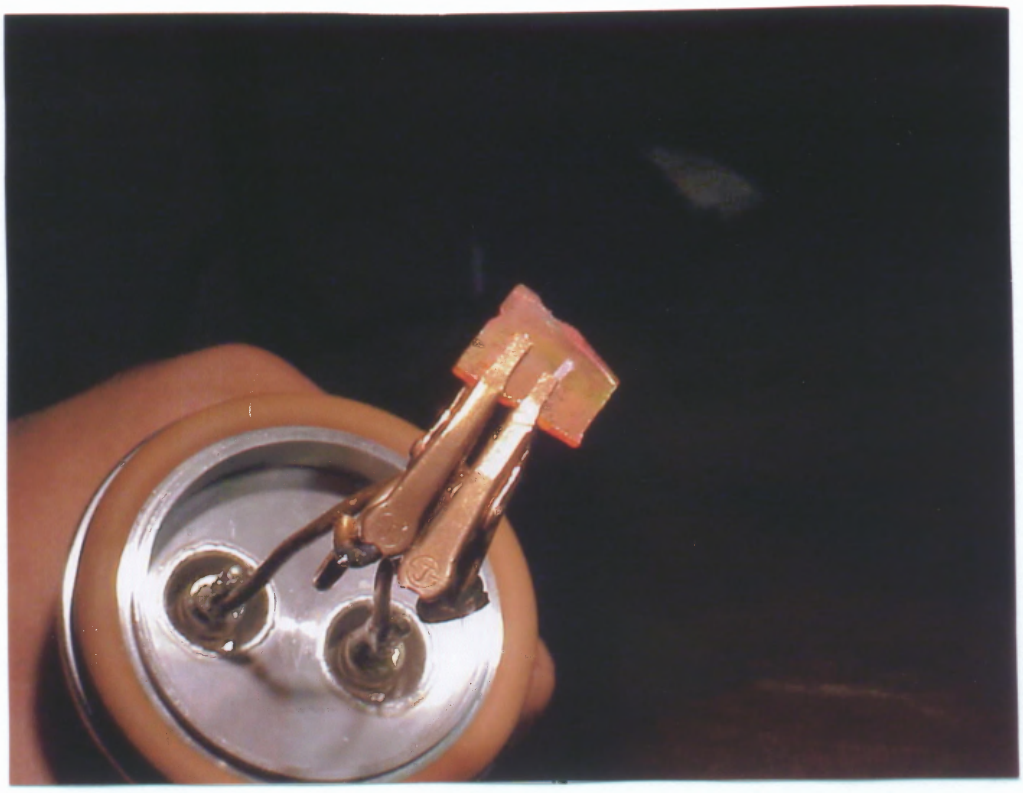

**Figure B.3** View of the dye coated sensor (SAMP sensor).

**Figure B.4** View of Experimental Apparatus II. The distance of the light source from the filter is approximately 2.5 inches.

## REFERENCES


1. Janata Jirí, *Principles of Chemical Sensors*, Plenum Press, New York, 1989

2. Diamond D., *Principles of Chemical and Biological Sensors*, Wiley Interscience Publication, New York, New York, 1998.

3. Mulchandani A., Sadik O. A., *Chemical and Biological Sensors for Environmental Monitoring*, American Chemical Society, Washington, D.C., 2000.

4. Taylor R.F., Schultz J. S., *Handbook of Chemical and Biological Sensors*, Institute of Physics Ltd., Philadelphia, Pennsylvania, 1996.

5. Zaitsev V.B. , T.V. Panova, *" The use of Vibronic Phenomena in Adsorption phase for developing semiconductor gas-sensors "*, Applied Surface Science, volume 167, pp 184-190, 2000.

6. Zaitsev V.B., Zotev A.V., Panova T.N., Plotnikov G.S., *The Effect of Adsorption on Photosensitized Conductivity of Thin Cadmium Sulfide Films.*", Chemistry and Physics Reports, Gordon and Breach Science Publishers, volume 18, pp. 1645-1651, 2000.

7. Cattrall R.W., *Chemical Sensors*, Oxford University Press Inc., New York, New York, 1997.

8. Miremadi B.K., Colbow K., Harima Y., "*A CdS photoconductivity gas sensor as an analytical tool for the detection and analysis of hazardous gases in the environment*", American Institute of Physics, 1997.